Small scale excess electron densities in the lower ionosphere of Mars:

Interpretation of Mars Express radio science observations in combination with MAVEN measurements

52th ESLAB symposium 2018, ESTEC, Netherlands

__K. Peter__[1], M. Pätzold[1], F. González-Galindo[2], L. Andersson[3], M. K. Bird[1,4], M. Crismani[3], C. M. Fowler[3], B. Häusler[5], D. Larson[6], R. Lillis[6], G. Molina-Cuberos[7], N. Schneider[3], S. Tellmann[1], O. Witasse[8]

[1] RIU Cologne, Cologne, Germany
[2] Instituto de Astrofísica de Andalucía, CSIC, Spain
[3] LASP, University of Colorado at Boulder, USA
[4] Argelander Institut für Astronomie, Bonn, Germany
[5] Univ. der Bundeswehr München, Germany
[6] SSL, Univ. of California, Berkeley, USA
[7] Universidad de Murcia, Murcia Spain
[8] ESA, ESTEC, The Netherlands

MaRS radio science

Figure adapted from S. Tellmann

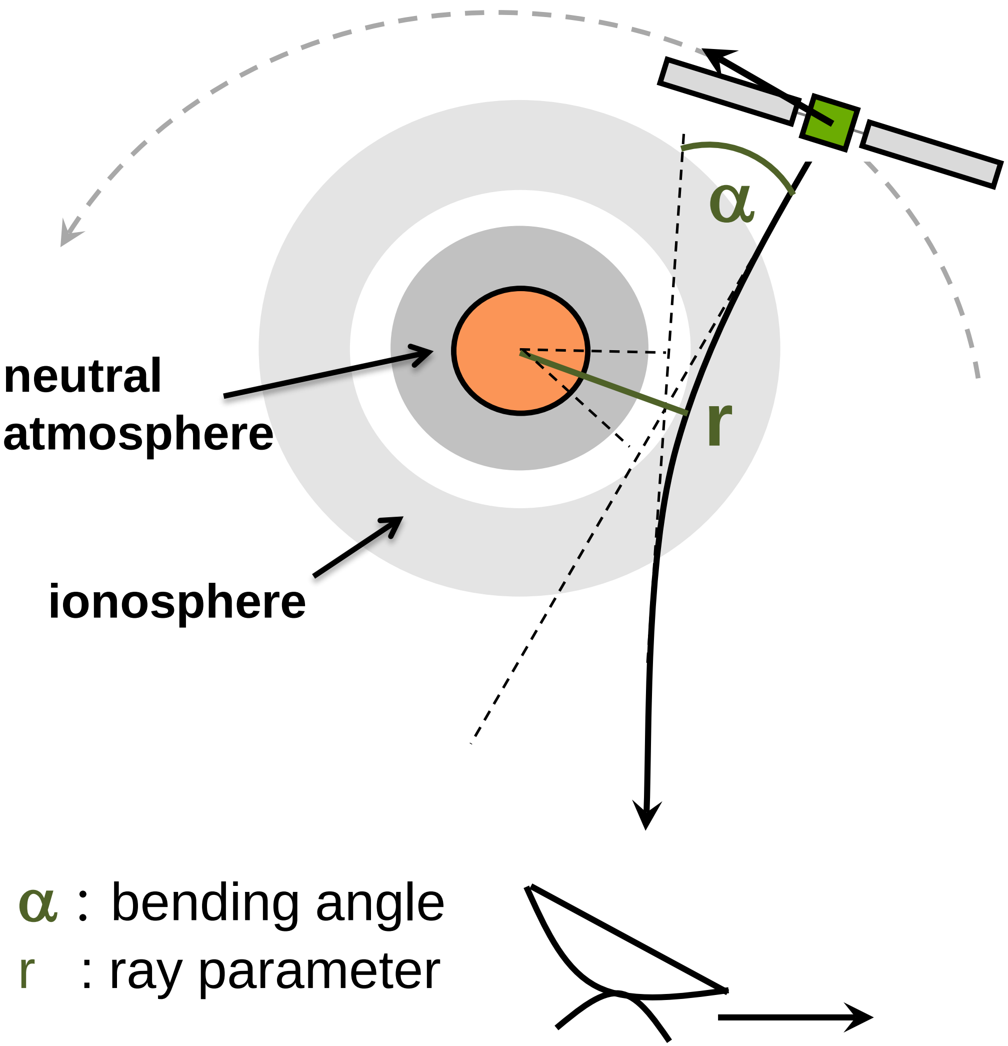

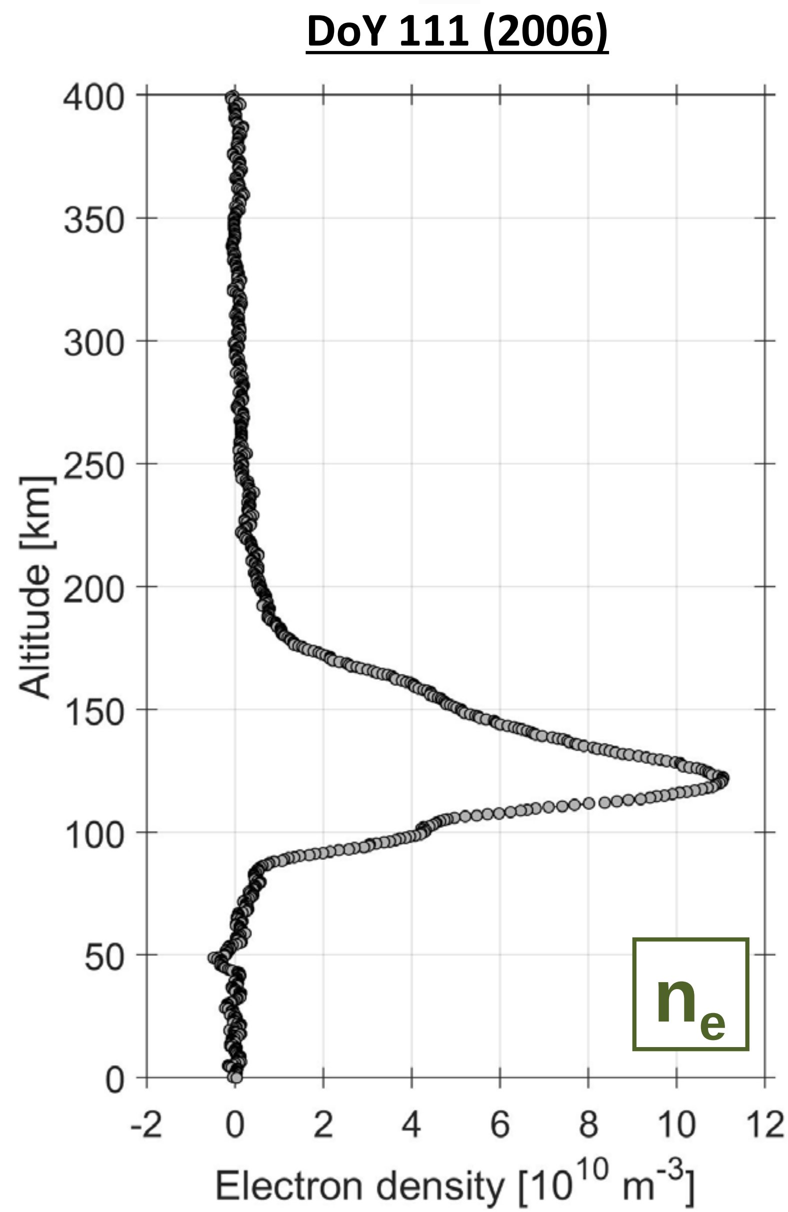

MEX-MaRS: excess electron density

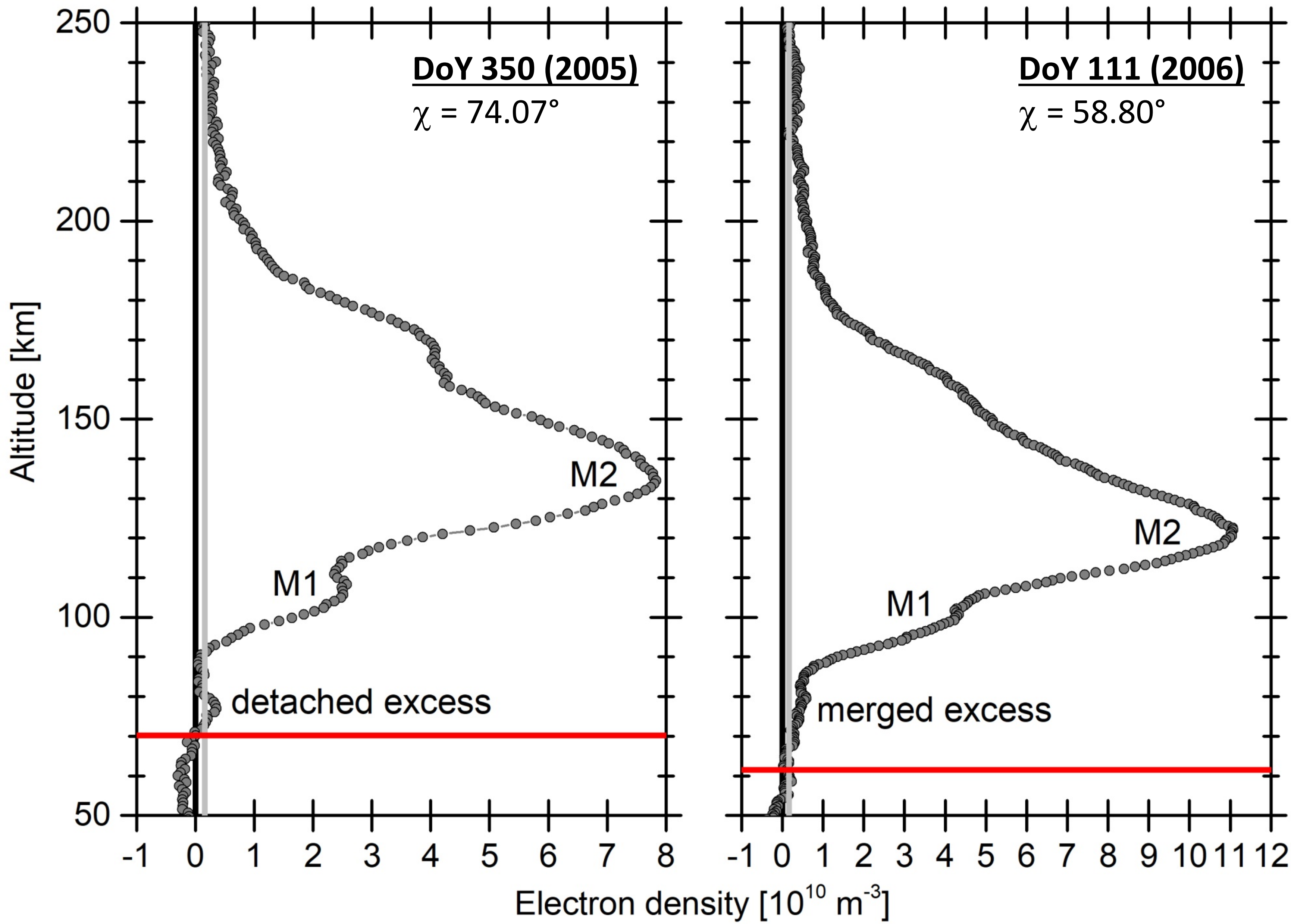

MEX-MaRS: excess electron density

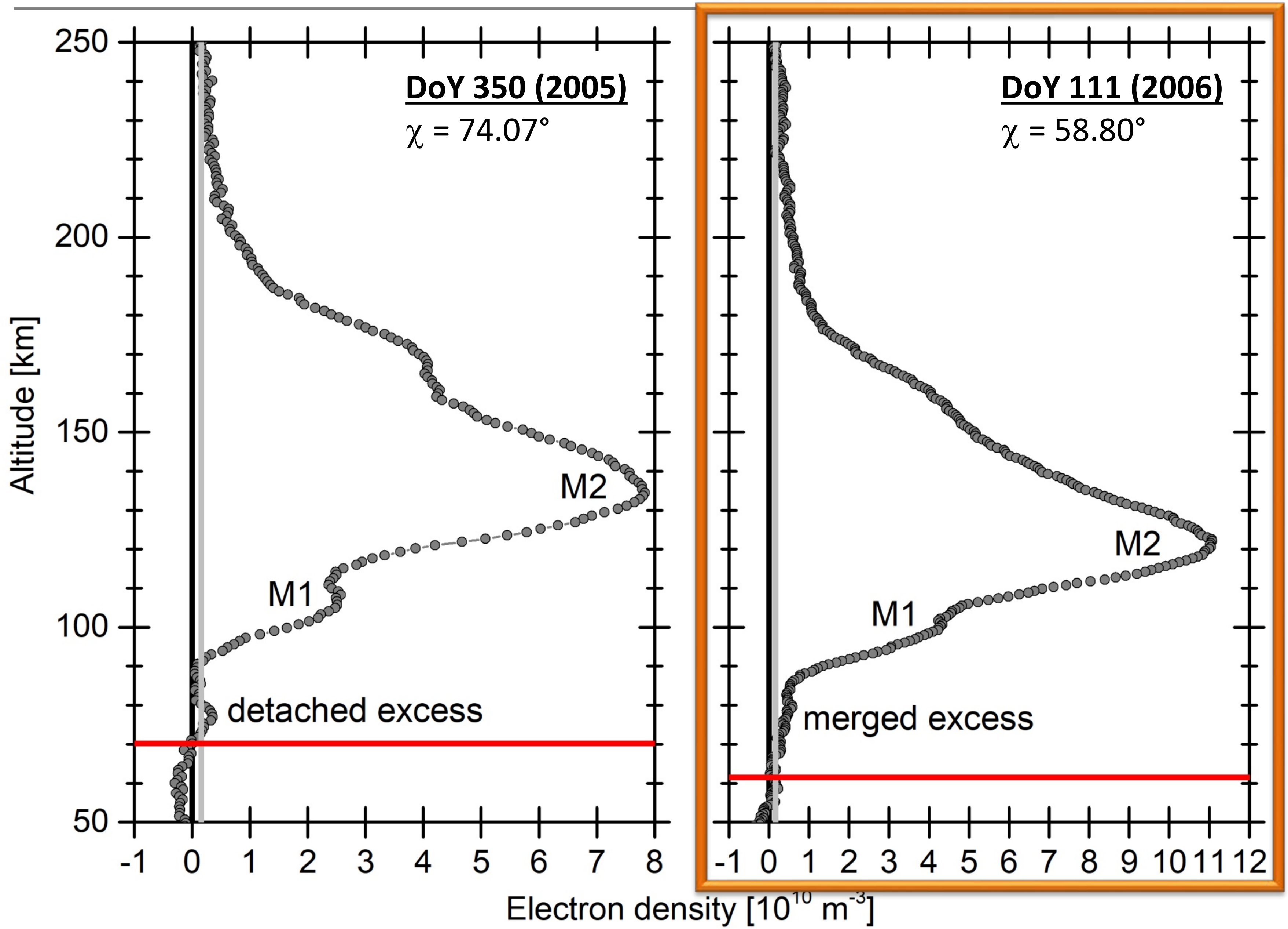

MEX-MaRS: excess electron density

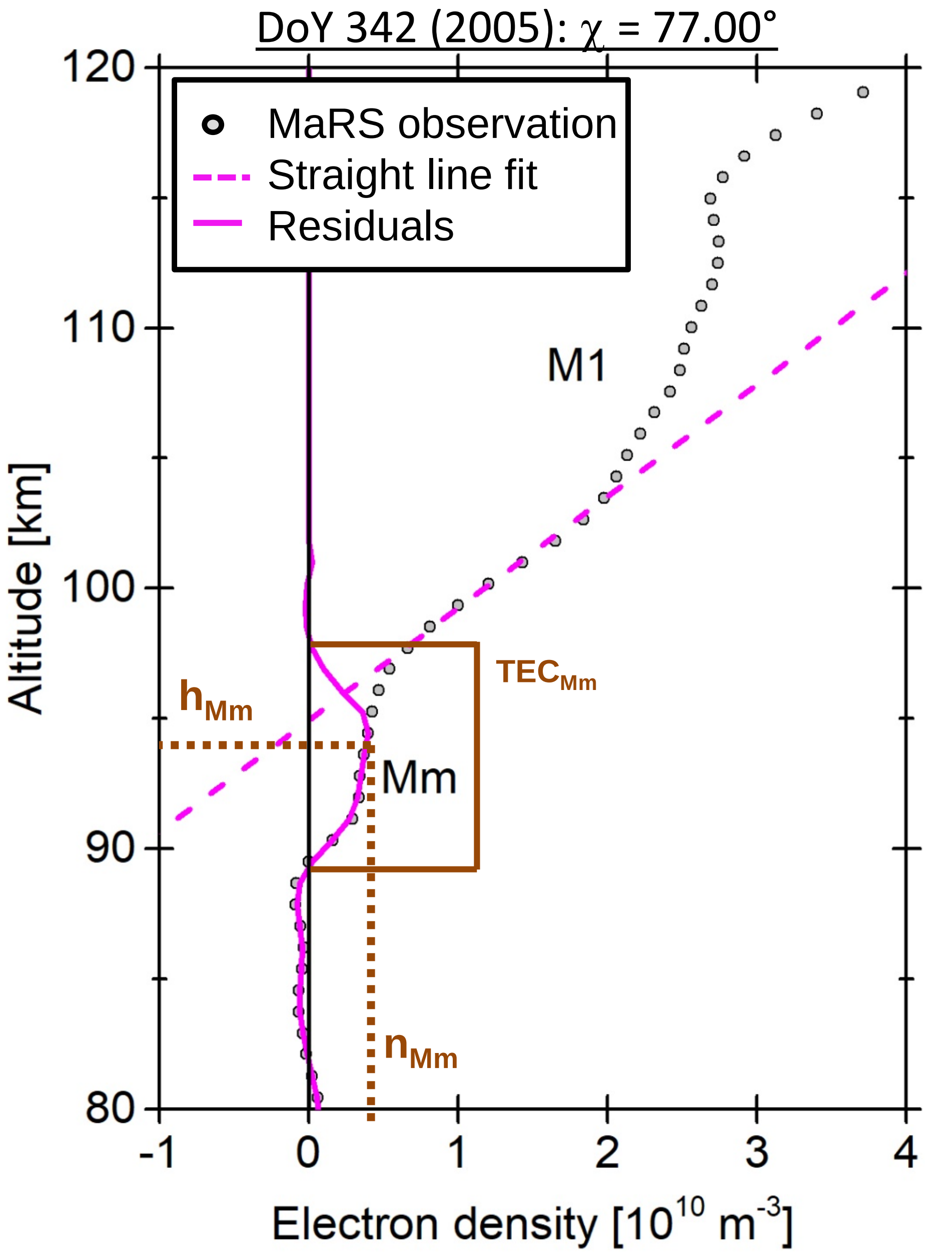

266 MaRS observations

- 2004 – **12/2014**
- solar zenith angle < 90°
- large scale noise level < $1.0 \circ 10^9$ m^{-3}

The Mm group contains all observations where

Mm TEC > 3000m∘3∘noise level.

Extracted Mm characteristics

n_{Mm} = peak residual el. density

h_{Mm} = altitude of n_{Mm}

TEC_{Mm} = integrated residual el. density

Mm: Solar zenith angle dependence

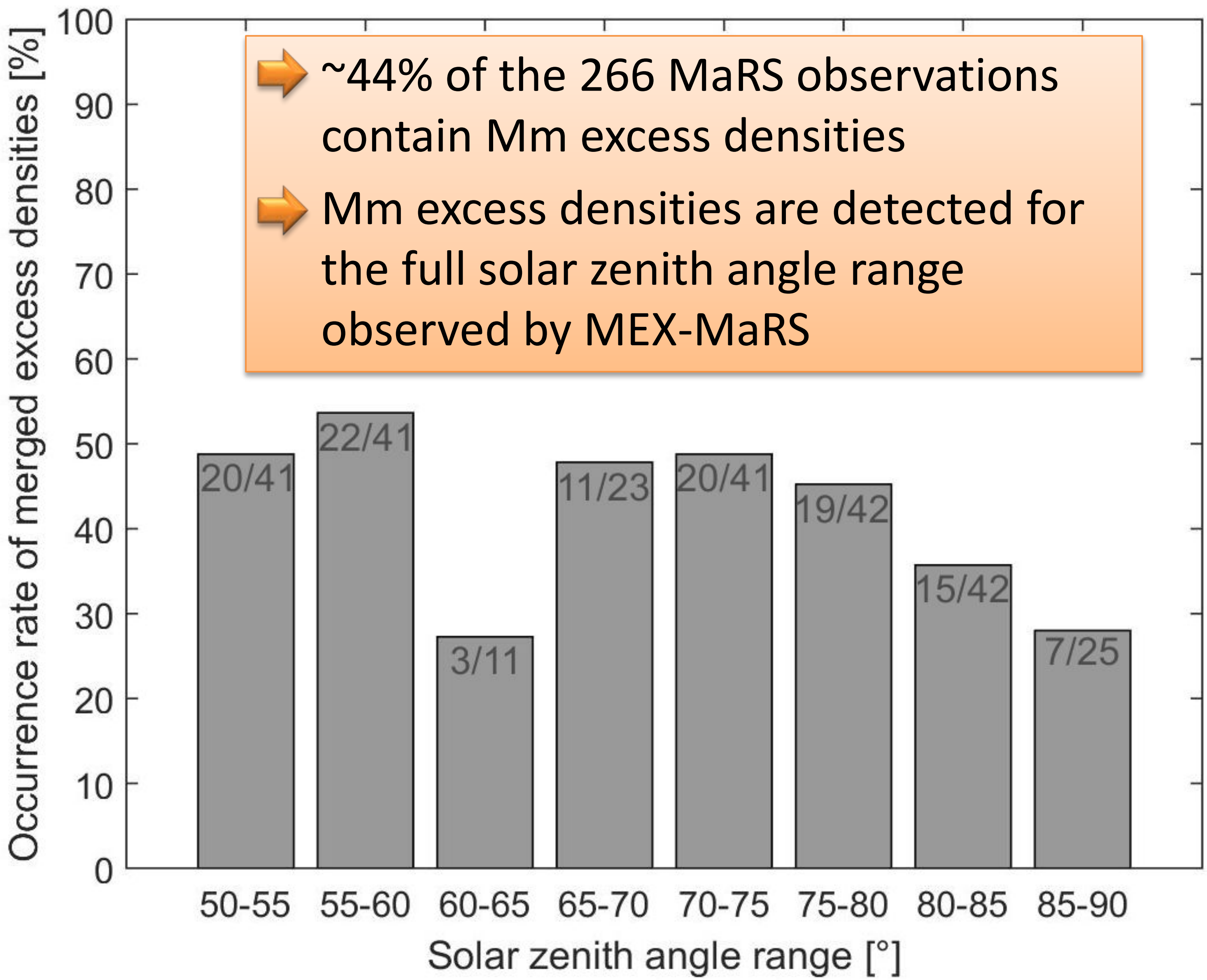

- ~44% of the 266 MaRS observations contain Mm excess densities
- Mm excess densities are detected for the full solar zenith angle range observed by MEX-MaRS

Mm: crustal magnetic field

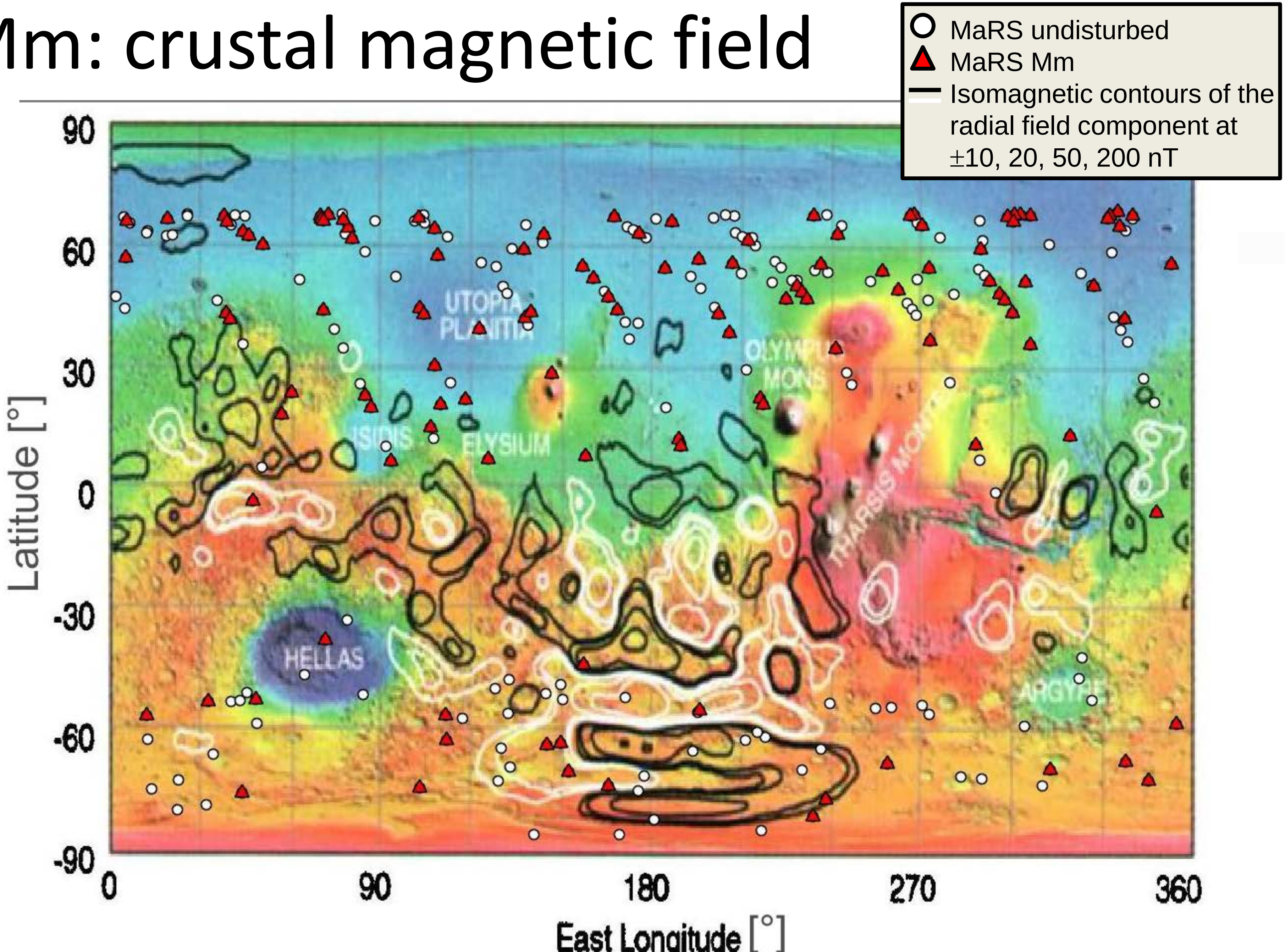

B_{rad} in 400 km altitude from MGS MAG/ER observations, *Connerney et al. 2001*

Mm: crustal magnetic field

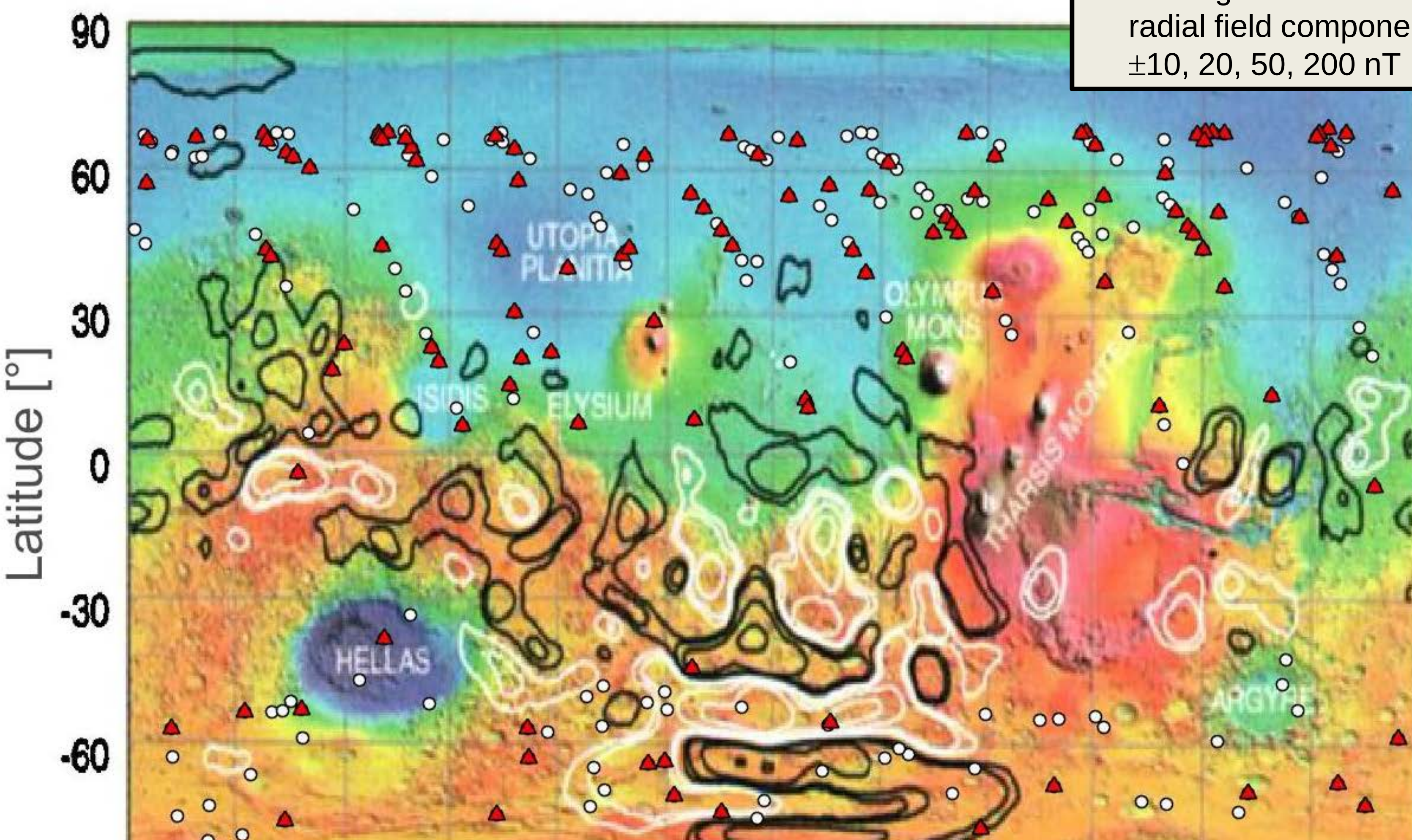

- MaRS data inconclusive concerning Mm occurrence rate dependence on high crustal magnetic fields
- Mm layers are available above regions with low crustal magnetic field

Mm: altitude of lower base

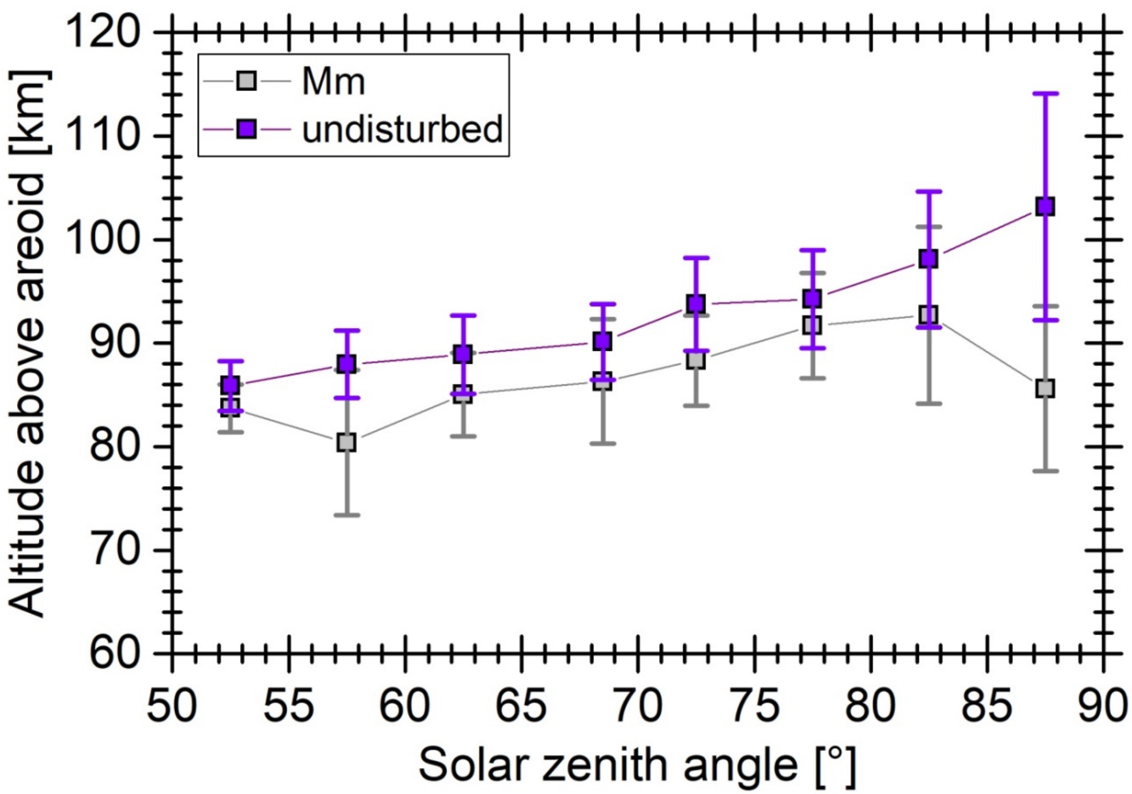

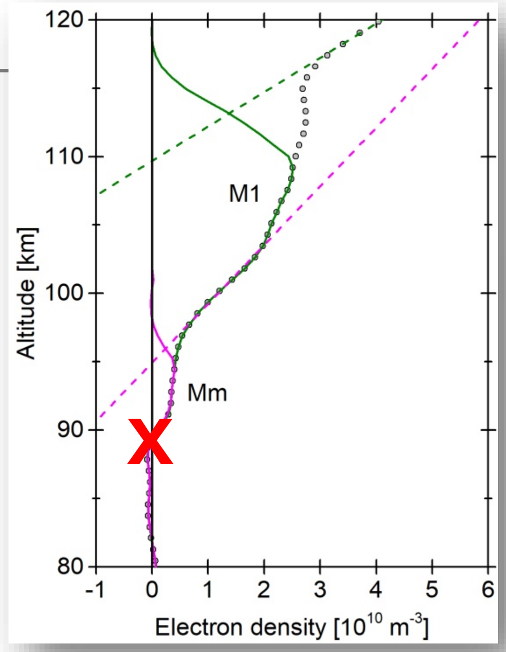

- The averaged ionospheric base with Mm observations is found at lower altitudes than the undisturbed ionospheric base.
- Strong correlation between Mm occurrence rate and SIP solar activity *(not shown)*
- Neither the full profile TEC, nor the M1 TEC is significantly affected by the physical processes causing Mm *(not shown)*.

Possible Mm origins are SEPs or short solar X-ray flux.

Mm: meteoric material

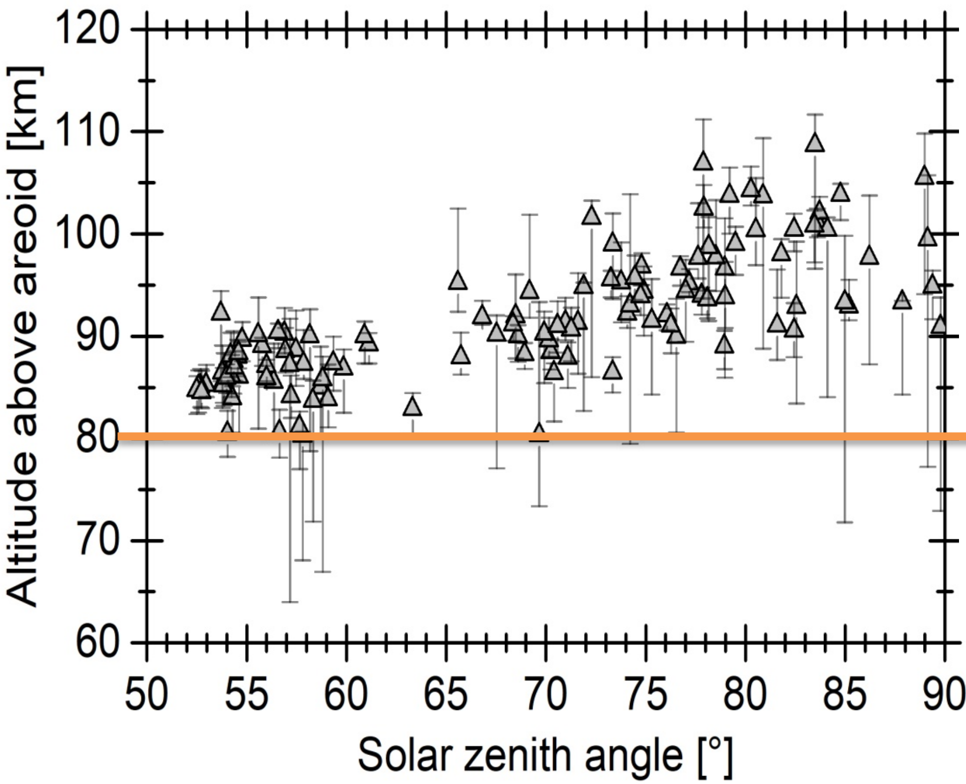

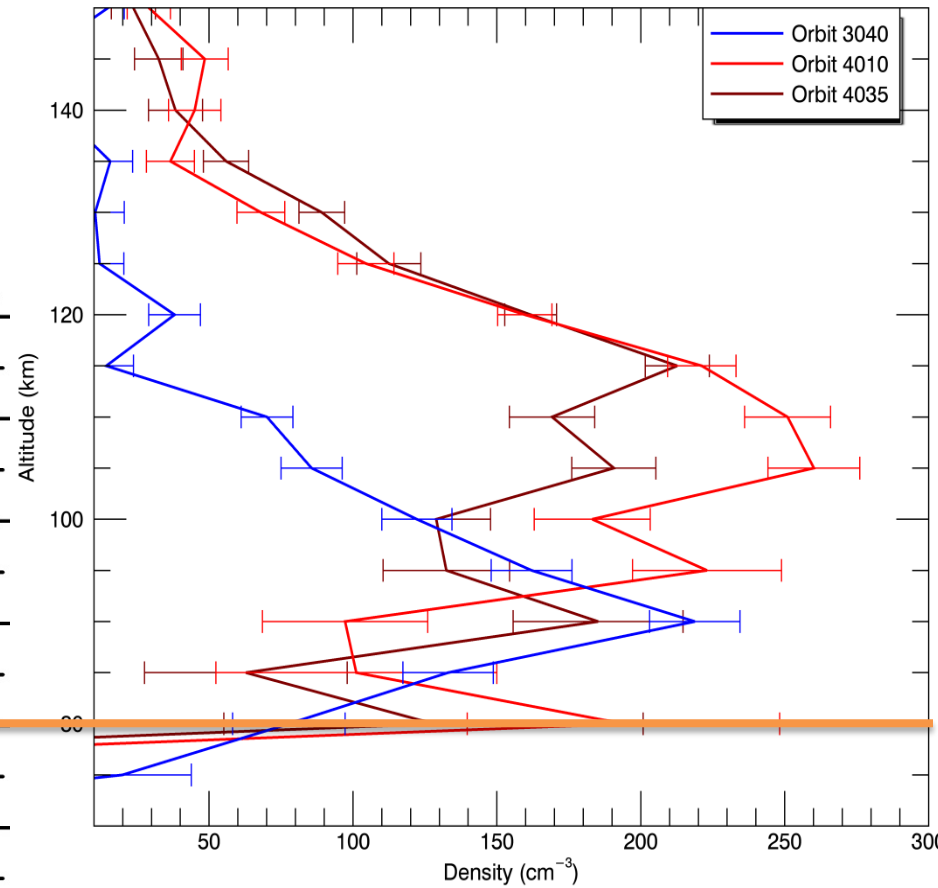

Mg⁺ densities observed by MAVEN IUVS

Crismani et al., MAVEN PSG 2016

Mm: meteoric material

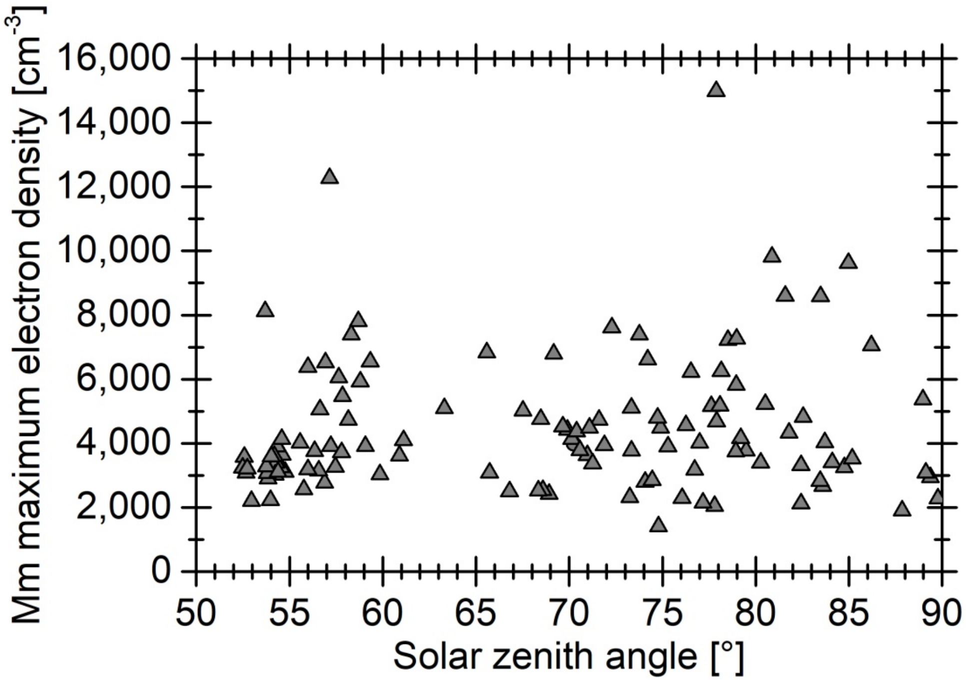

Mg$^+$ densities observed by MAVEN IUVS

Crismani et al., MAVEN PSG 2016

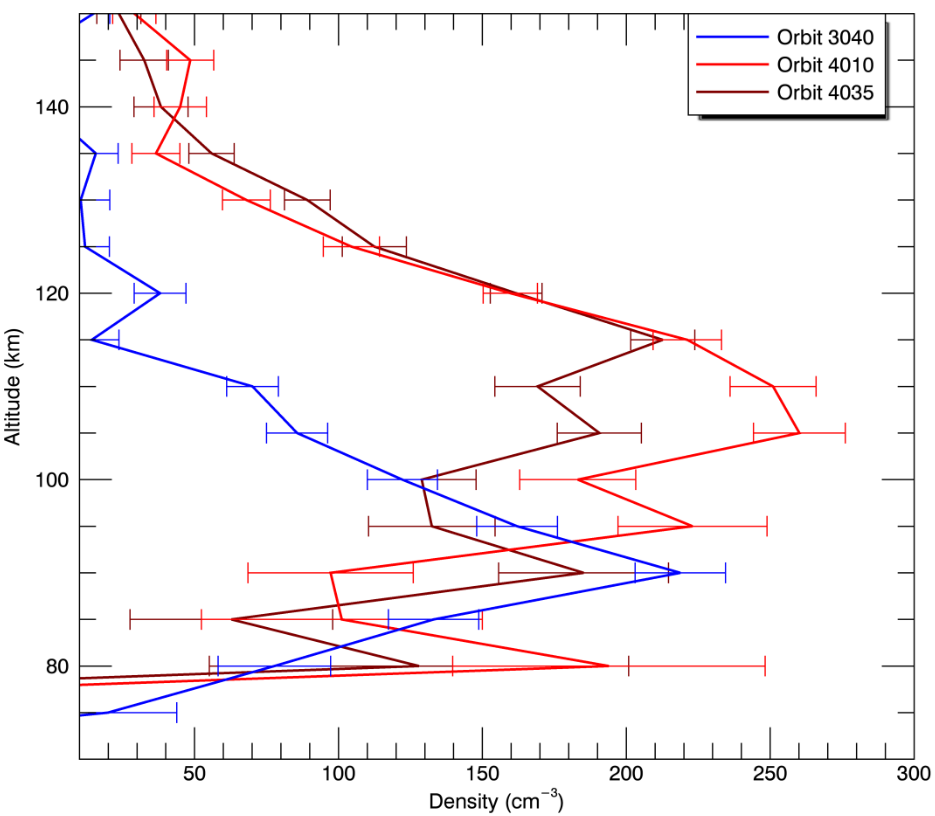

- The MAVEN IUVS detects Mg^+ densities lower than $1{\circ}10^9$ m^{-3}.
  Crismani et al., Nature Geoscience 2017

➡ This is lower than the lowest detected Mm maximum electron density.

	IonA-2
Type	1D time-stepping photochemical model with diurnal cycle
Input neutral atmosphere	Mars Climate Database V5.2, 24h variable neutral temperature and atmosphere *CO_2, N_2, O, O_2, O_3, H_2O, H, H_2, Ar, CO*
Input electron temperatue	Electron temperature from *Rohrbough et al., (1979)* derived from Viking lander in-situ observations
Solar radiation	Solar2000 V2.38, *Tobiska et al. (2000)*
Solar flux cross sections	*Huebner and Mukherjee (2015),* *except for O_3 (Sander et al., 2011) and* *CO_2 and N_2 (individual calculation from several sources)*
Secondary ionization	W-value approach, *Wedlund et al. (2011)*
Reaction scheme	*Gonzalez-Galindo et al. (2013), Fox and Sung (2001),* *Fox (2012), Fox (2015)*
Neutral transport	Minor molecular diffusion *C, H_2O_2, HO_2, O(^{1}D), N(^{2}D), N, NO, NO_2, OH*
Ion transport	Ambipolar diffusion (neutral-ion, ion-ion, ion-el. collisions) Ar^+, CO_2^+, CO^+, C^+, HCO_2^+, HCO^+, H^+, N_2^+, NO^+, N^+, O_2^+, O^+

IonA-2 solar flux 0.45 – 800 nm
Model start at 9 LST

DoY 336, 2005
χ = 78.78°

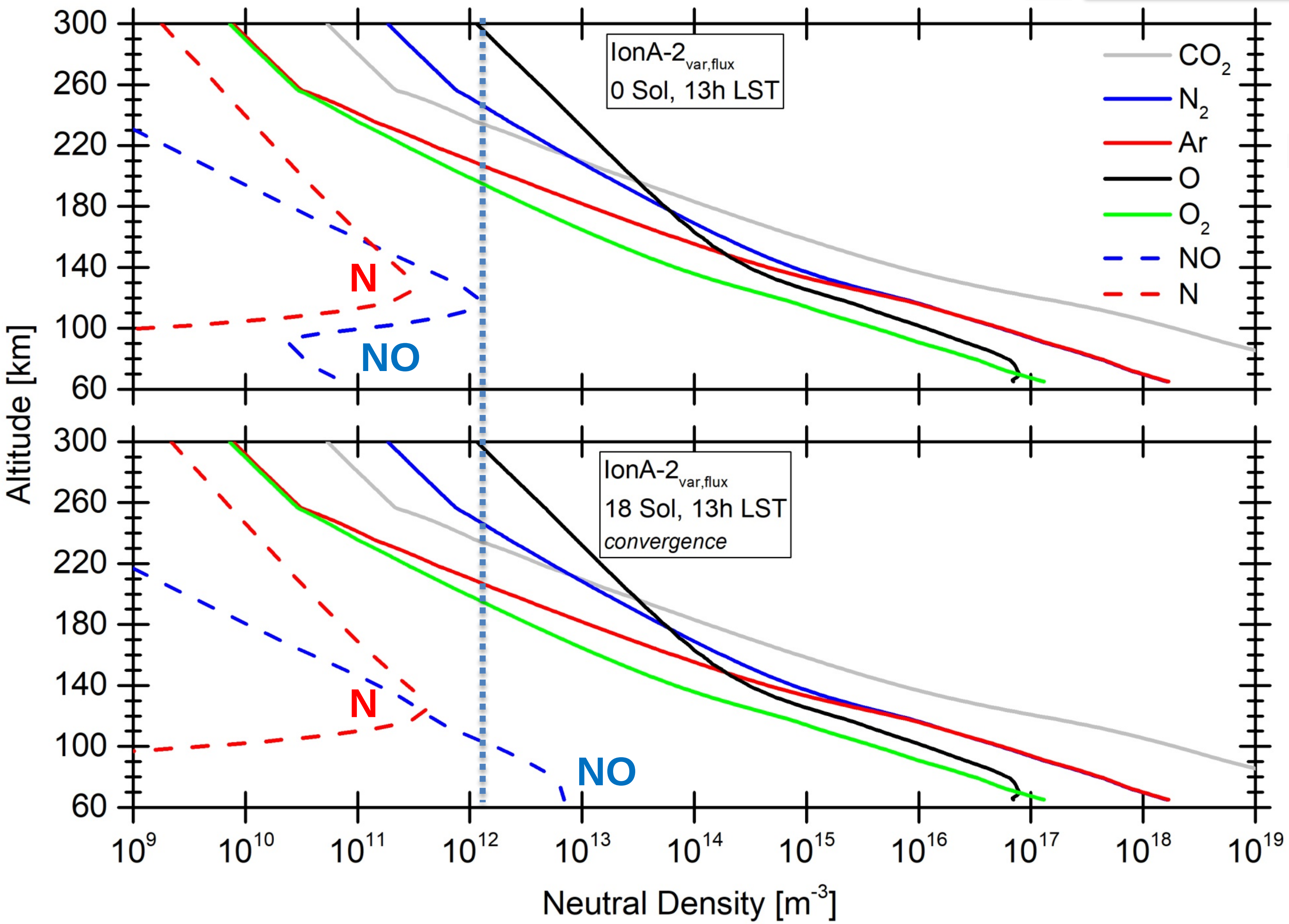

IonA-2 solar flux 0.45 – 800 nm
Model start at 9 LST

DoY 336, 2005
χ = 78.78°

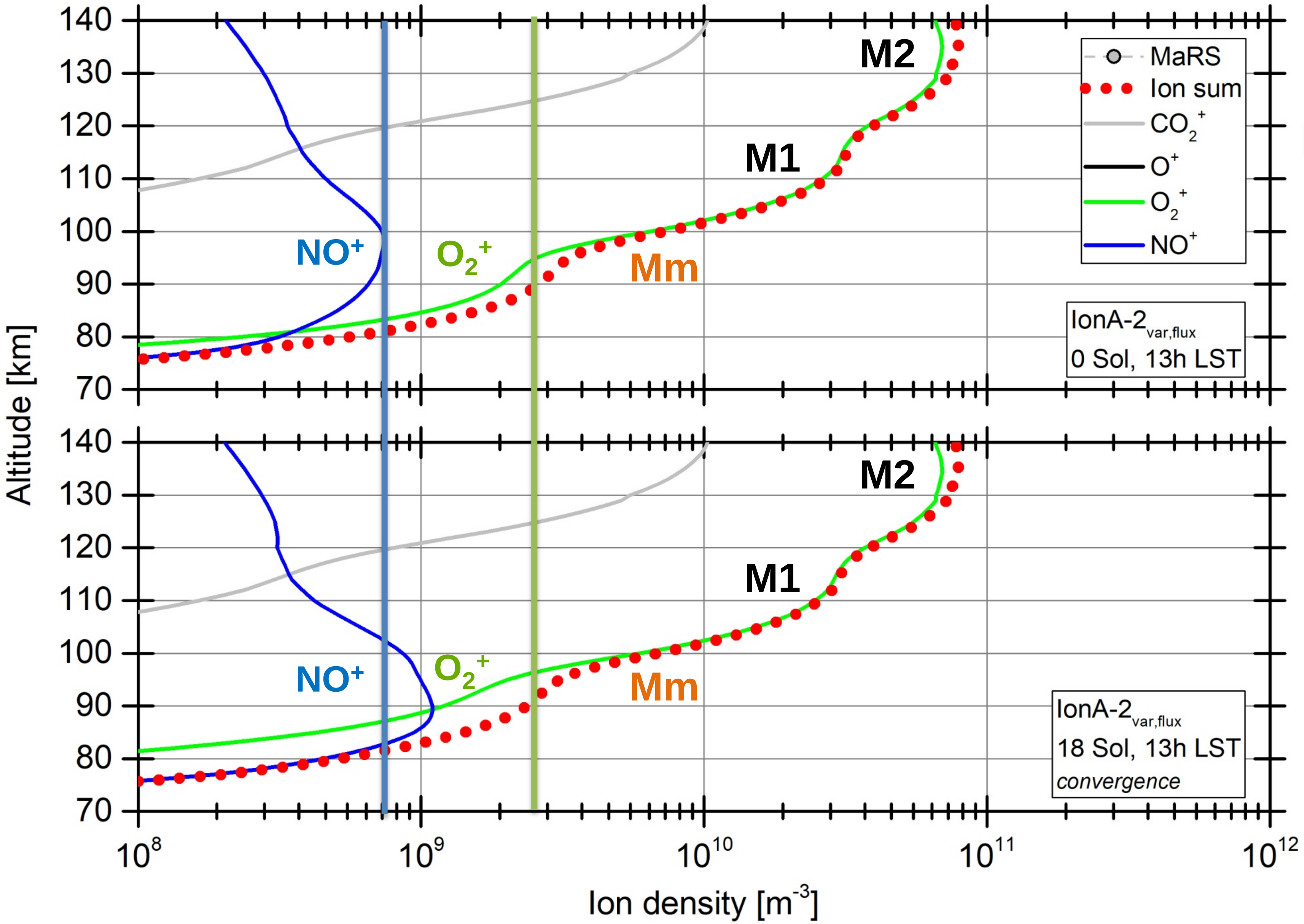

Mm: Local ions O_2^+ & NO^+

DoY 336, 2005
χ = 78.78°

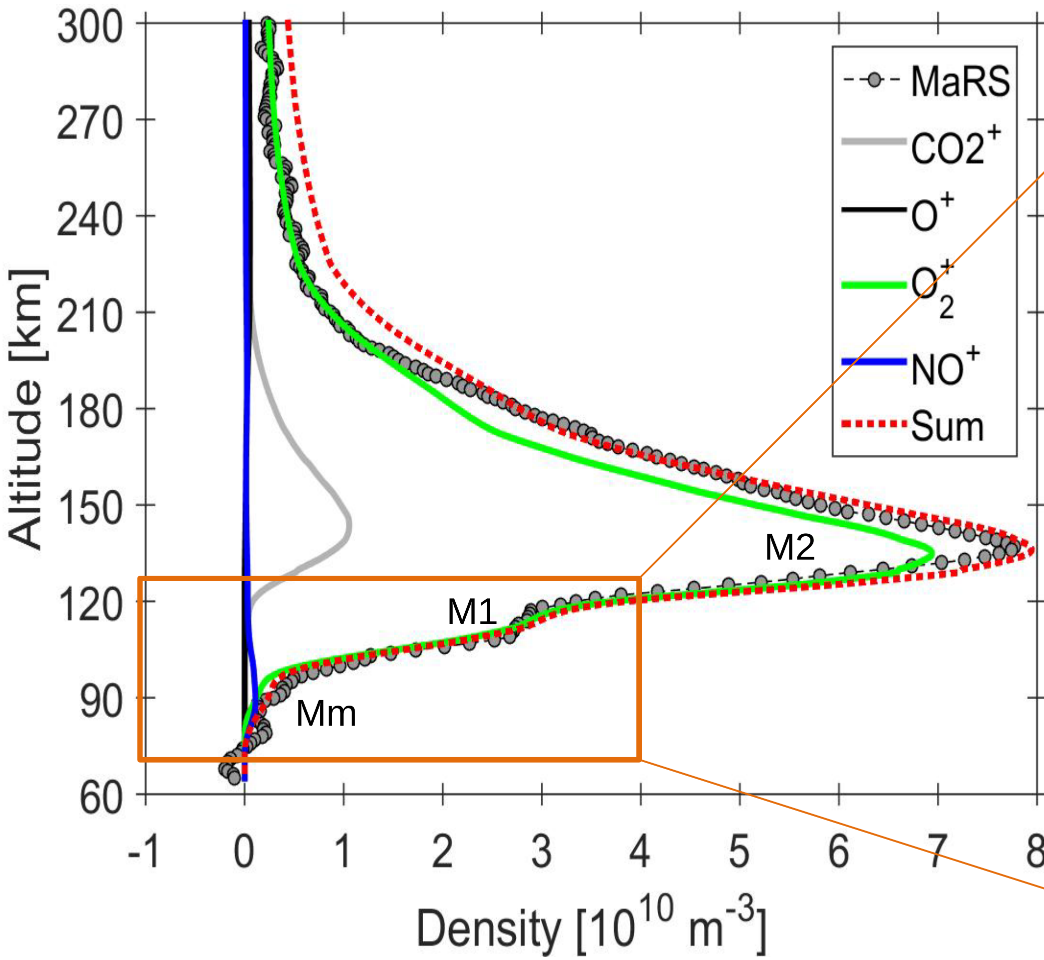

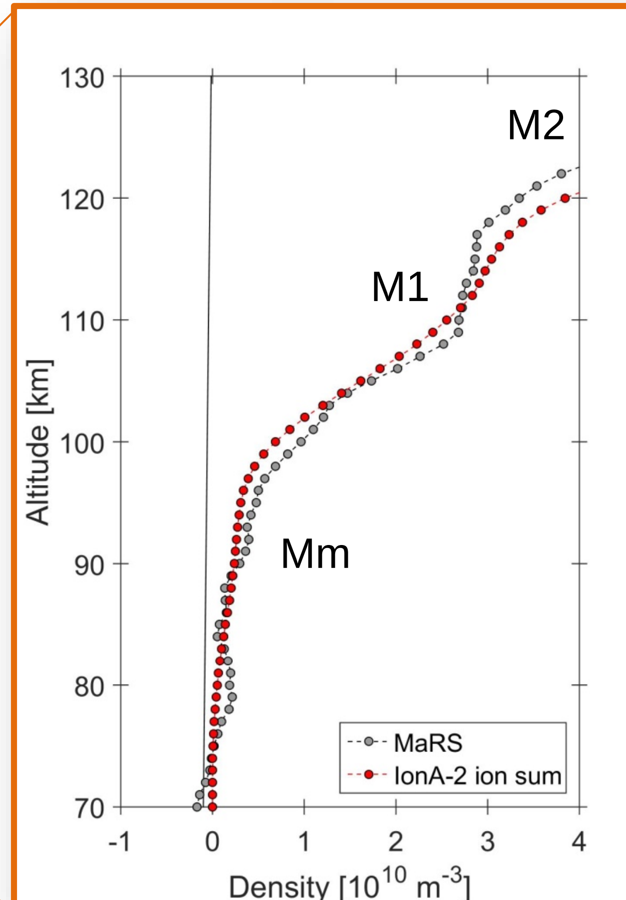

- NO density between 65 and 100 km determines the ratio between NO^+ and O_2^+.
- The model results reproduce the observed V-shaped Mm feature without artifical X-ray enhancement.

IonA-2 solar flux 0.45 – 800 nm
Model start at 9 LST

DoY 336, 2005
χ = 78.78°

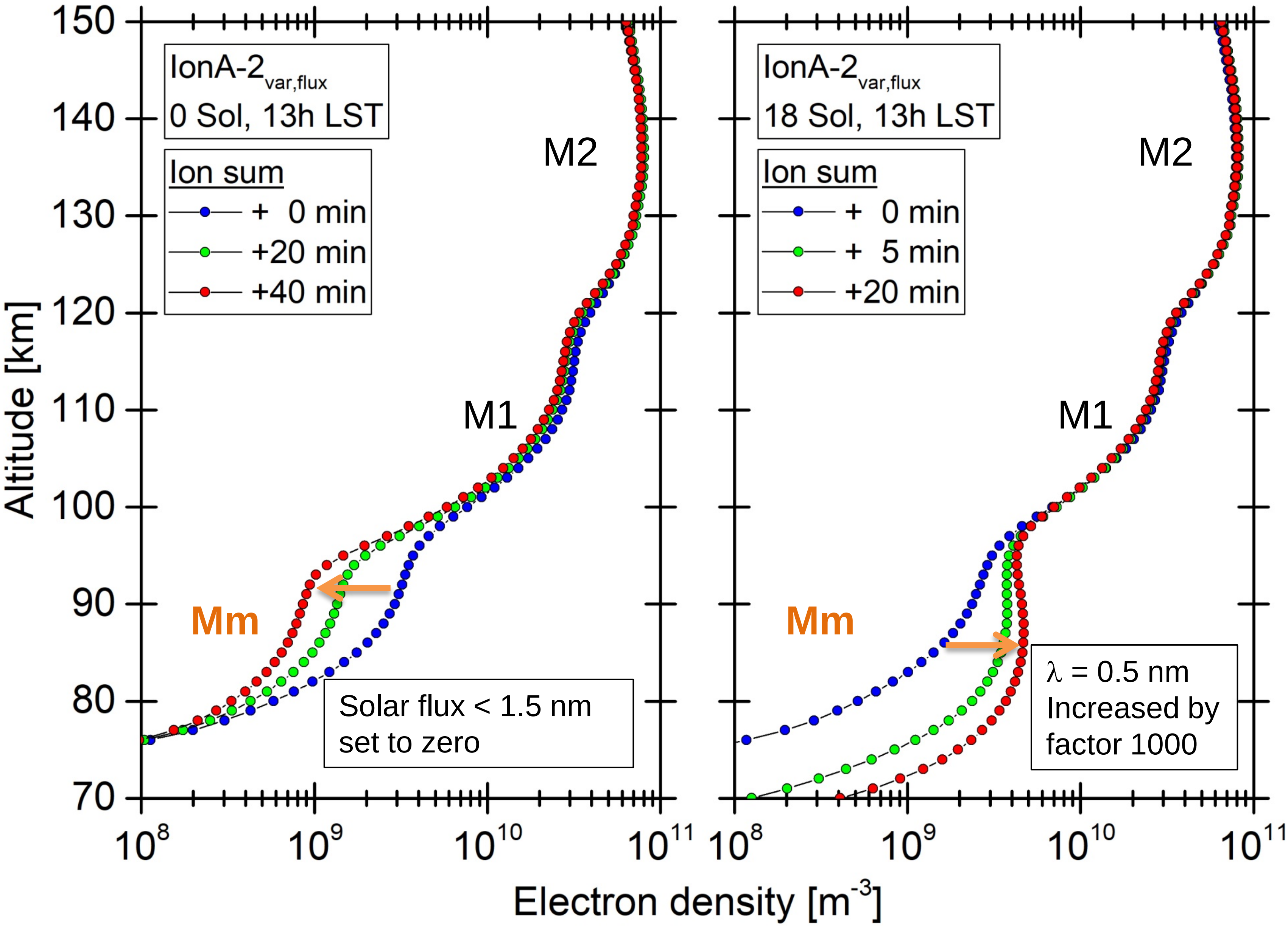

IonA-2 solar flux 0.45 – 800 nm
Model start at 9 LST

DoY 336, 2005
χ = 78.78°

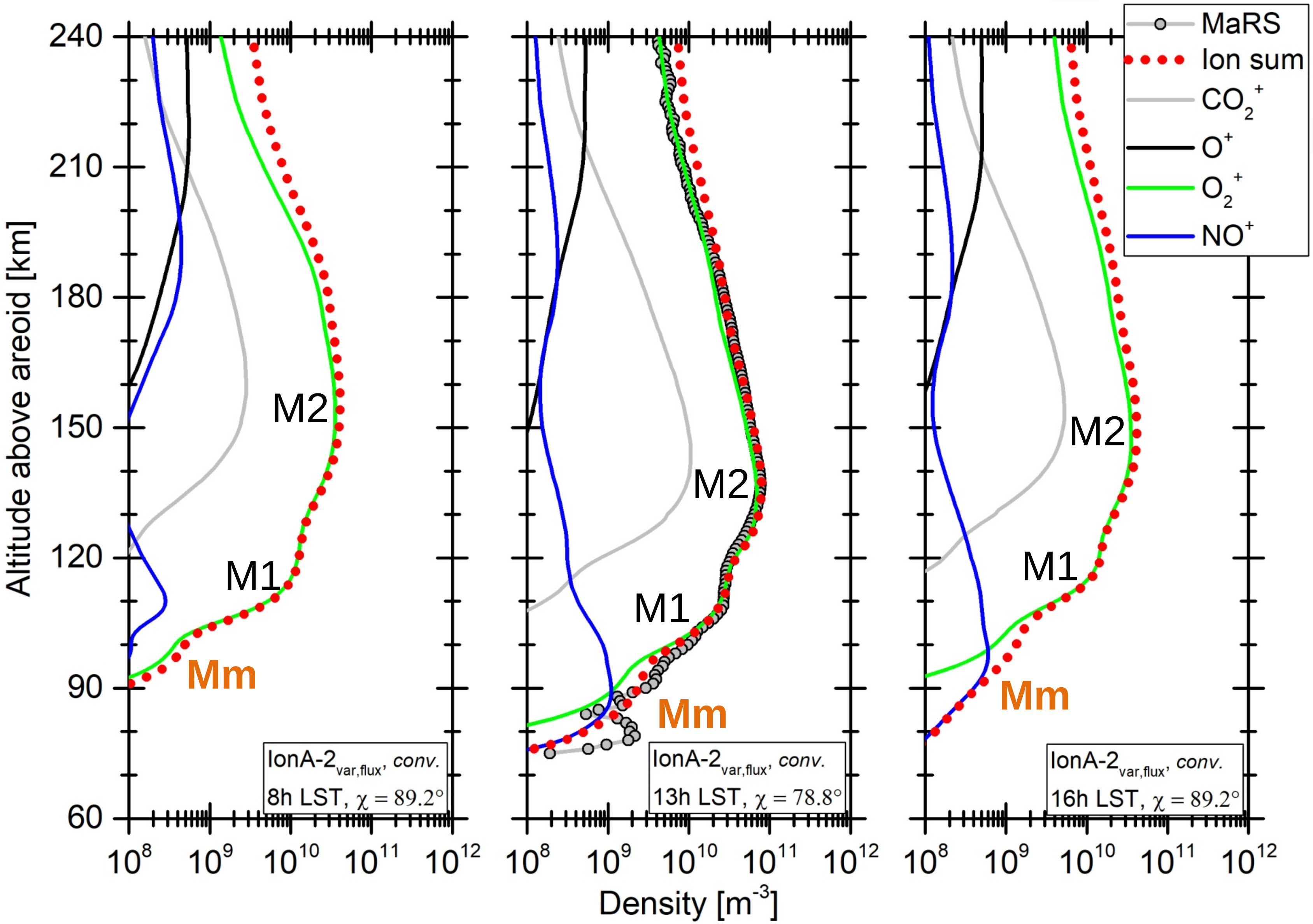

Comparison of MaRS OCC 2014 - 2017 with MVN-EUV av. model fluxes < 1nm

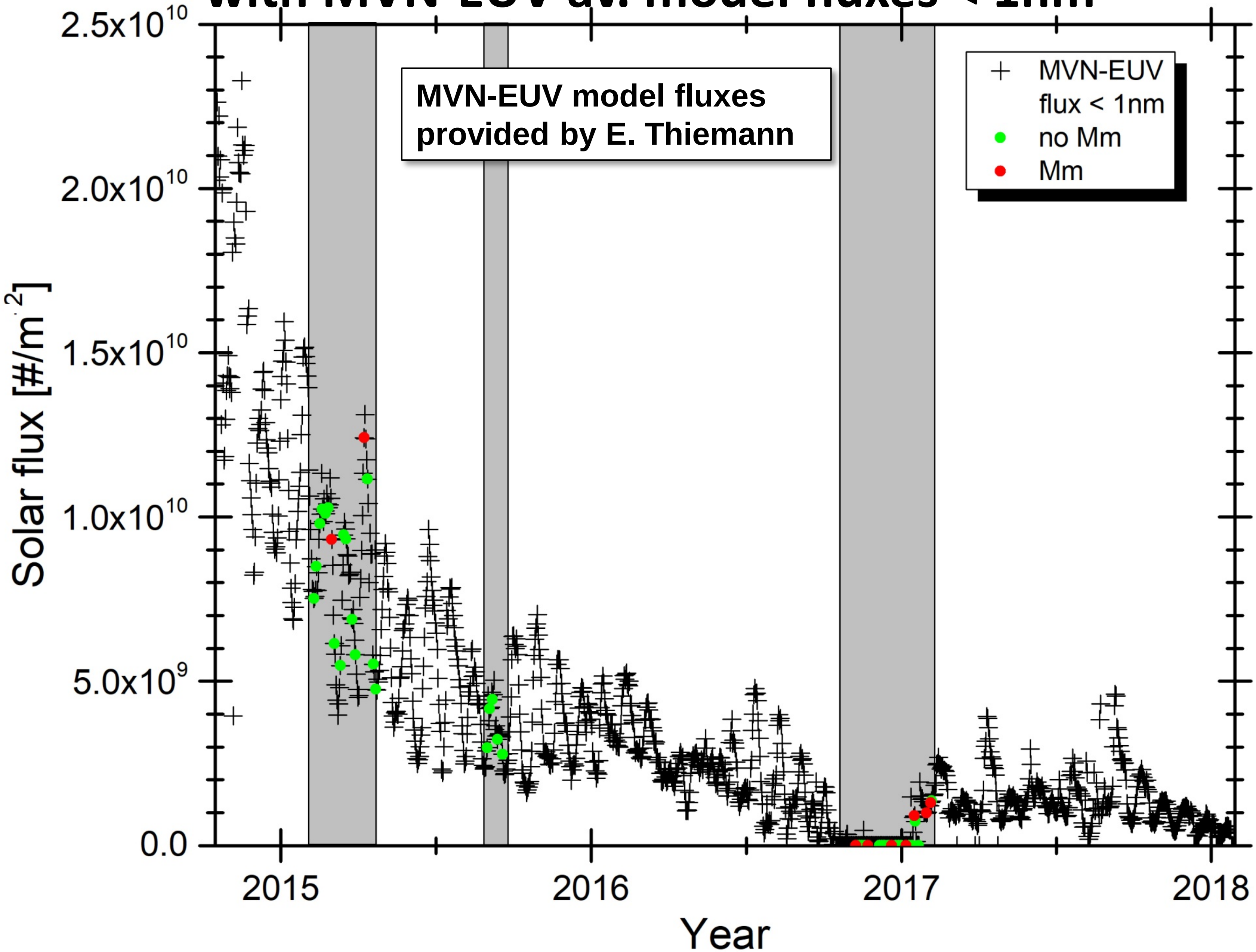

Comparison of MaRS OCC 2014 - 2017 with MVN-EUV av. model fluxes < 1nm

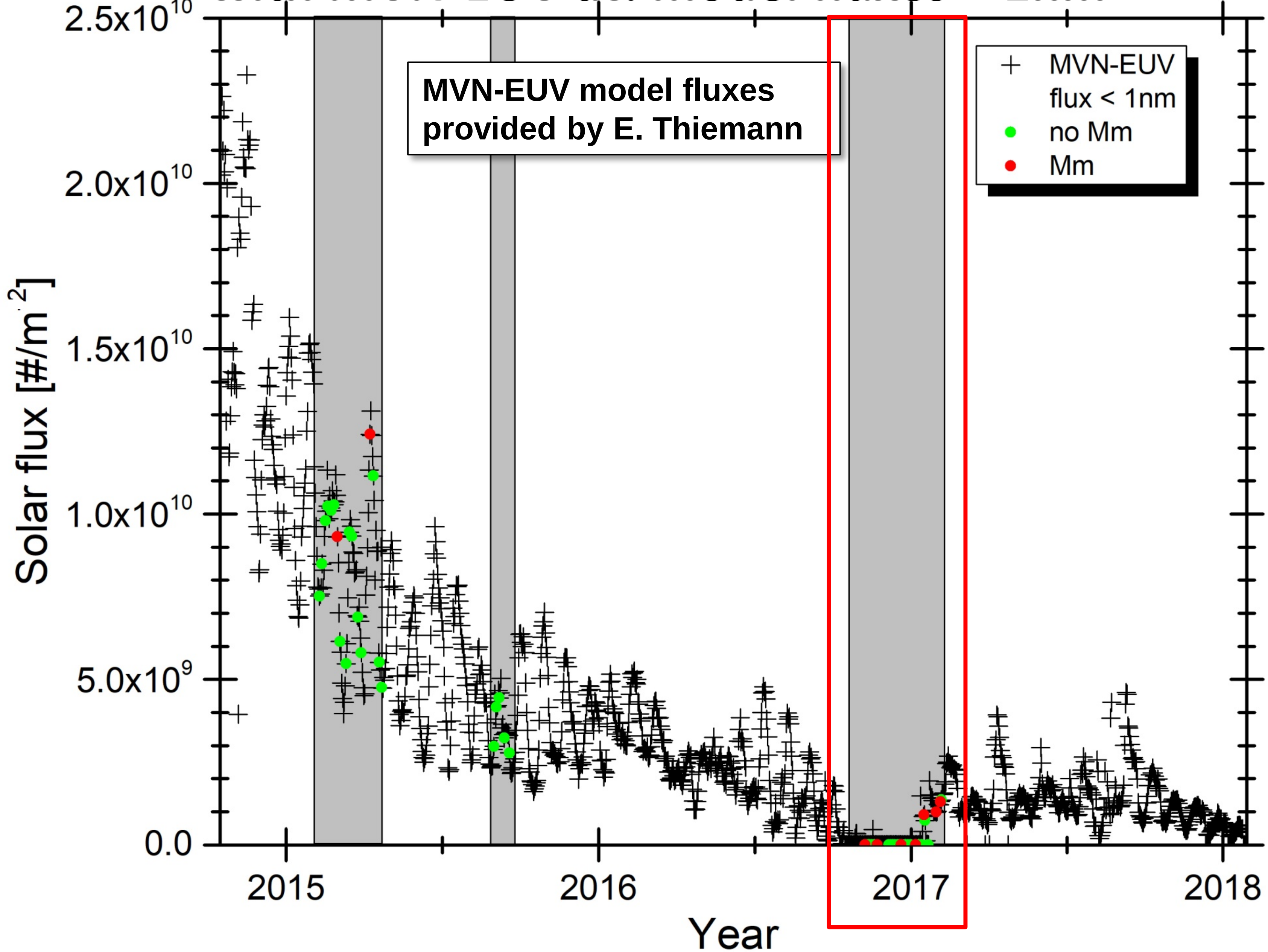

Comparison of MaRS OCC 2014 - 2017 with MVN-EUV av. model fluxes < 1nm

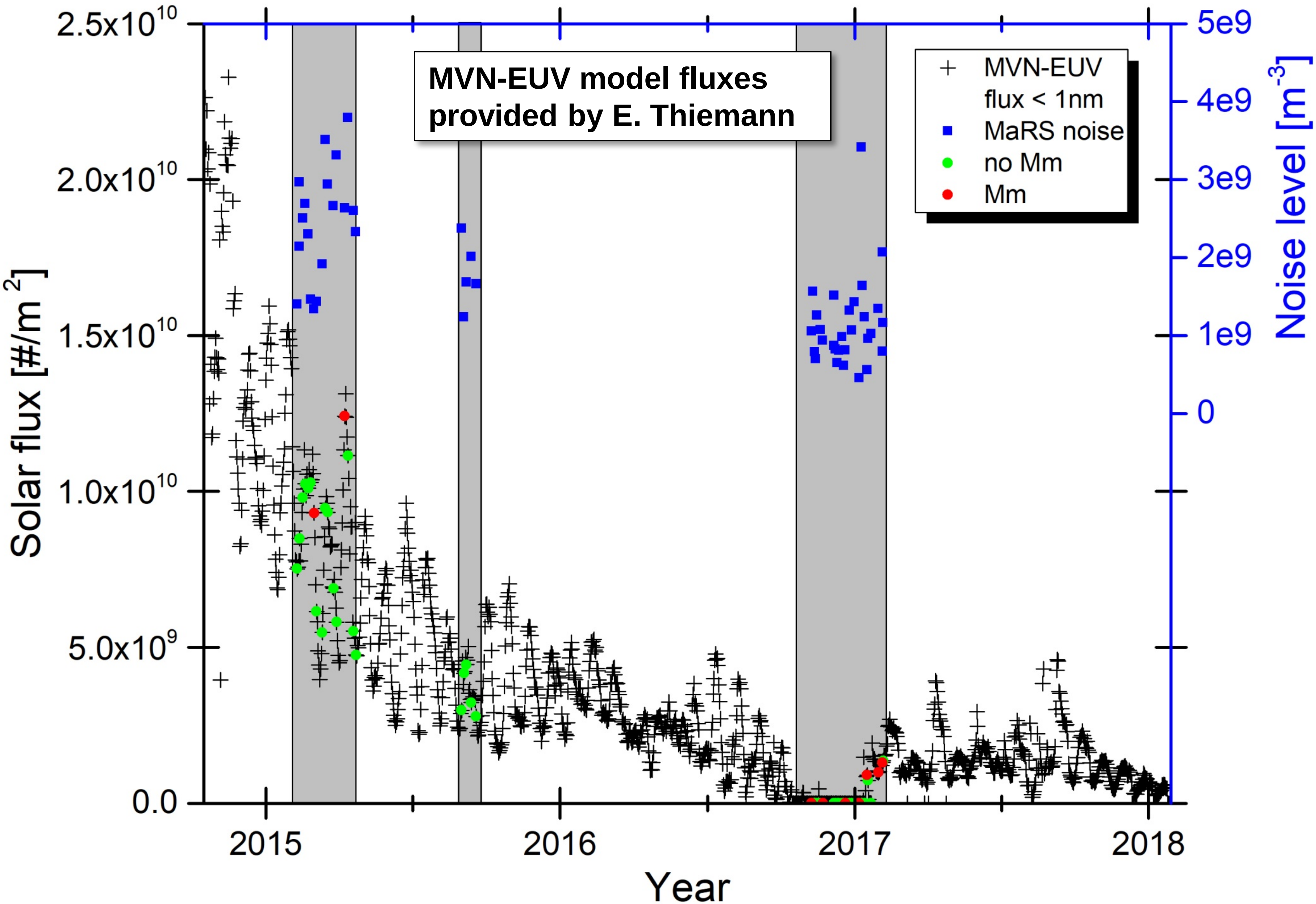

Comparison of MaRS OCC 2014 - 2017 with MVN-EUV av. model fluxes < 1nm

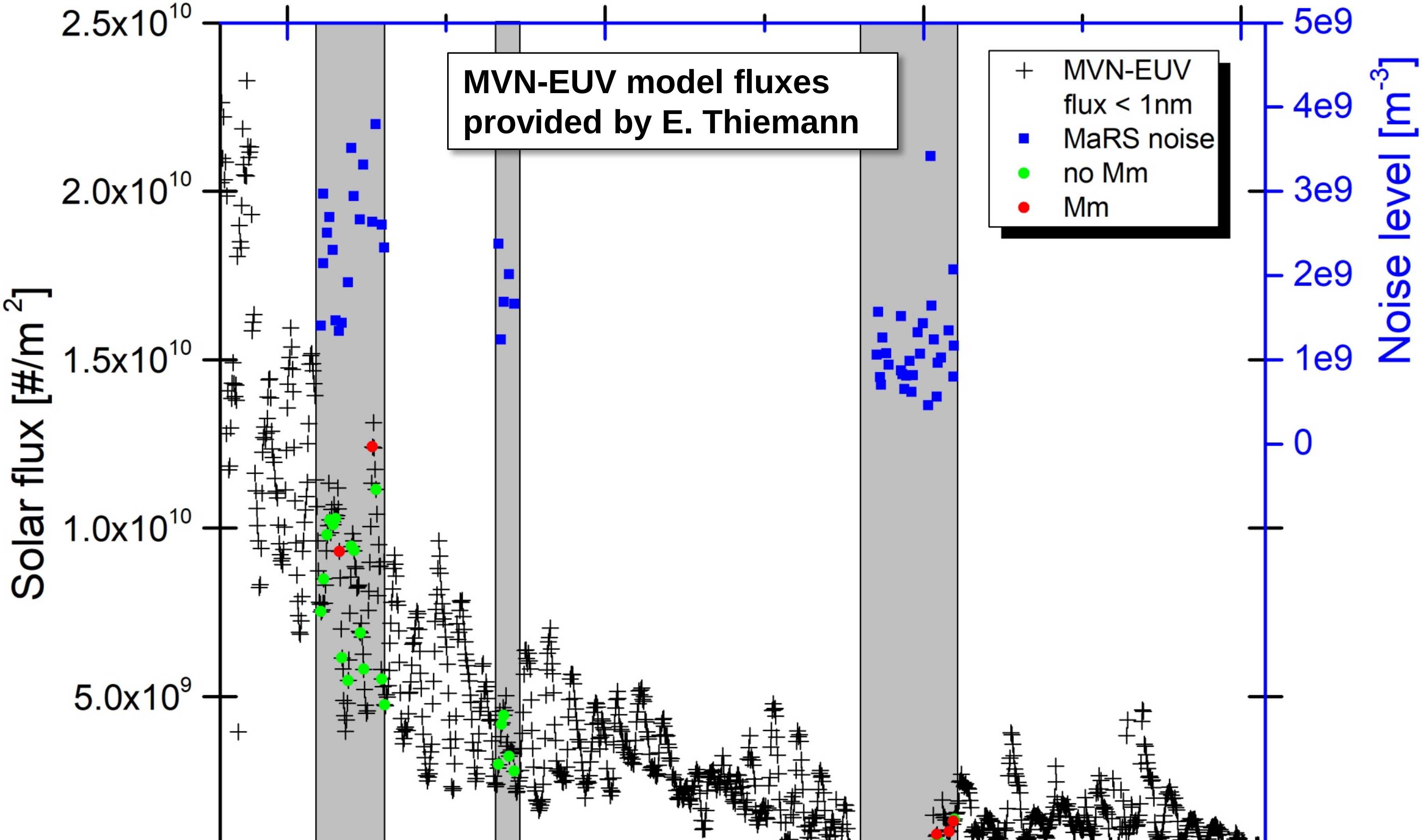

More MaRS observations are needed for the further investigation of the role of short solar X-ray in the formation process of the Mm.

Conclusions

- Implications from the MaRS observations
  - The Mm occurrences are less sporadic than expected.
  - The observed MAVEN IUVS Mg^+ density is too small to be the only responsible ion species for the identified Mm.
  - Wind shear is an unlikely process for the formation of the observed Mm.
  - Short solar X-ray (<1.5 nm) or SEPs are the most probable energy source for the ionization in the Mm altitude range between 70 and 110 km.

Conclusions

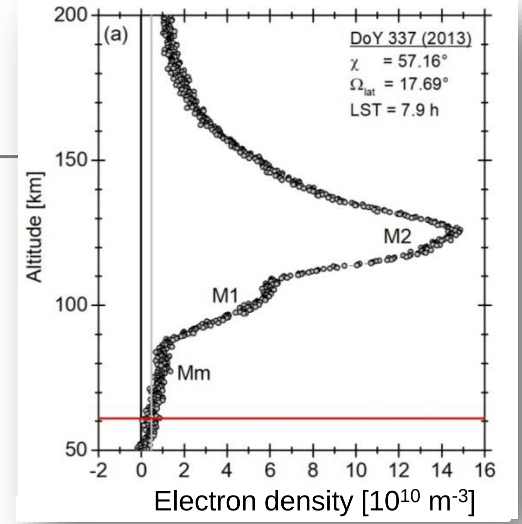

- Implications from the IonA-2 model
  - The ionization of ambient atmospheric ions (O_2^+, NO^+) by short solar X-ray provides an excellent agreement with the V-shaped Mm.
  - The model Mm vertical TEC, peak electron densities and altitudes are in excellent agreement with the observed Mm characteristics.
  - The sporadic occurrence of the Mm is explained by a combination of observational (e.g. noise level) and environmental (e.g. variable solar flux) parameters.
  - Additional sources might provide additional electron density (Mg^+), additional substructures (gravity waves) or strong Mm enhancements with large ionospheric disturbances (SEP events).
- Implications from first comparisons with MAVEN-EUV model data
  - More MaRS observations are needed for the further investigation of the role of short solar X-ray in the formation process of the merged excess electron densities.

Backup slides

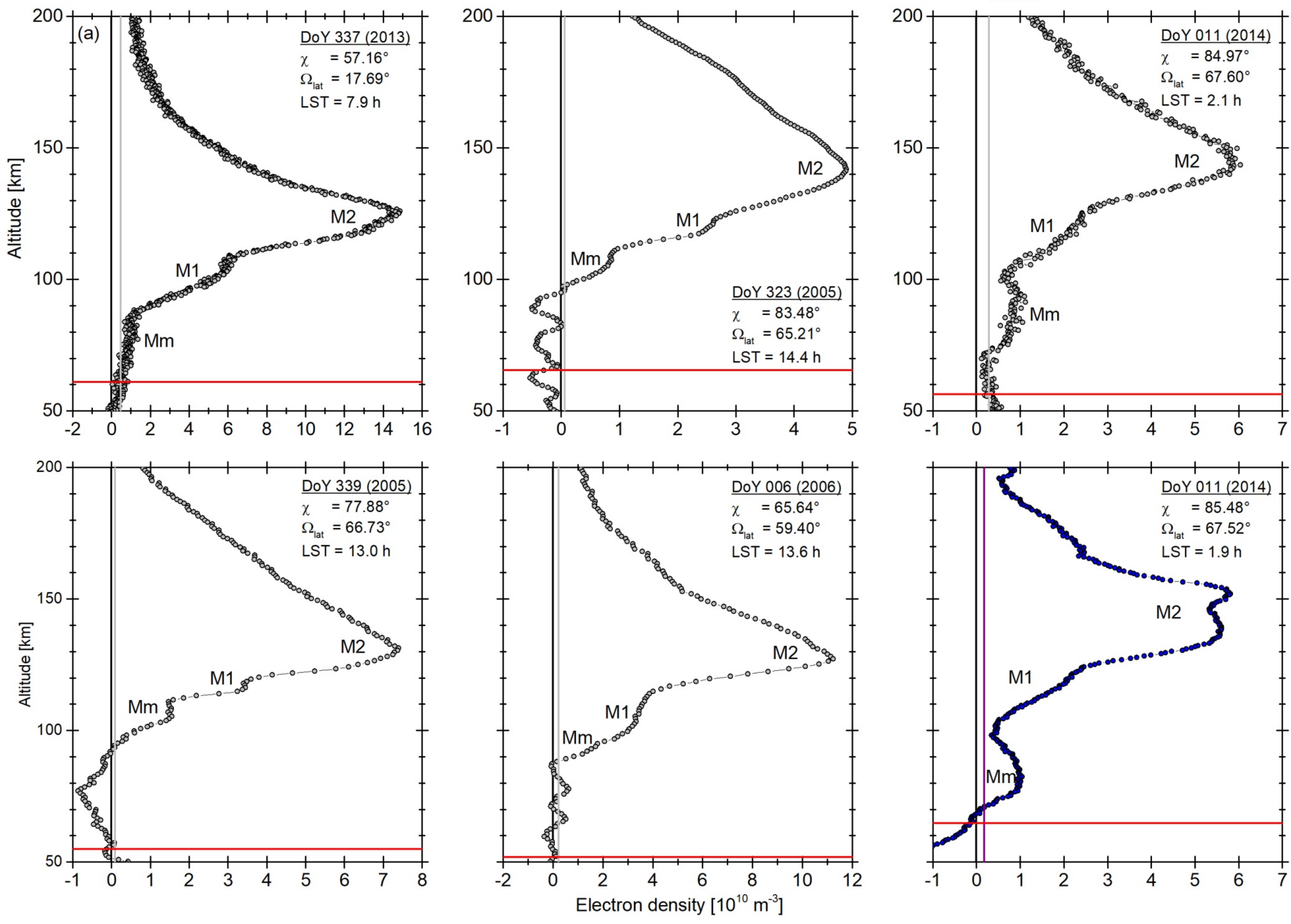

(a)
DoY 337 (2013)
χ = 57.16°
Ω_lat = 17.69°
LST = 7.9 h
M2
M1
Mm
DoY 323 (2005)
χ = 83.48°
Ω_lat = 65.21°
LST = 14.4 h
M2
M1
Mm
DoY 011 (2014)
χ = 84.97°
Ω_lat = 67.60°
LST = 2.1 h
M2
M1
Mm
DoY 339 (2005)
χ = 77.88°
Ω_lat = 66.73°
LST = 13.0 h
M2
M1
Mm
DoY 006 (2006)
χ = 65.64°
Ω_lat = 59.40°
LST = 13.6 h
M2
M1
Mm
DoY 011 (2014)
χ = 85.48°
Ω_lat = 67.52°
LST = 1.9 h
M2
M1
Mm
Altitude [km]
Electron density [10^10 m^-3]

MaRS observational results

- ~44% of the 266 MaRS obs. contain Mm excess densities
  - ➡ **Mm occurrence is less sporadic than expected**

- Most observed Mm appear over low crustal magnetic fields
  - ➡ **Wind shear mechanism unlikely for the observed Mm**

- The Mm base is on average found at lower altitudes compared to the undisturbed MaRS profiles.
- Strong correlation of the Mm occurrence rate with the Suns activity.
- Neither the full profile TEC, nor the M1 TEC is significantly affected by the physical processes causing Mm.
  - ➡ **Short solar X-ray or SEPs are needed for the primary ionization process in the altitude range of 70 – 110 km.**
  - Potential ions
    - Meteoric material (Mg^+)
    - Local ionospheric ions (O_2^+, NO^+)

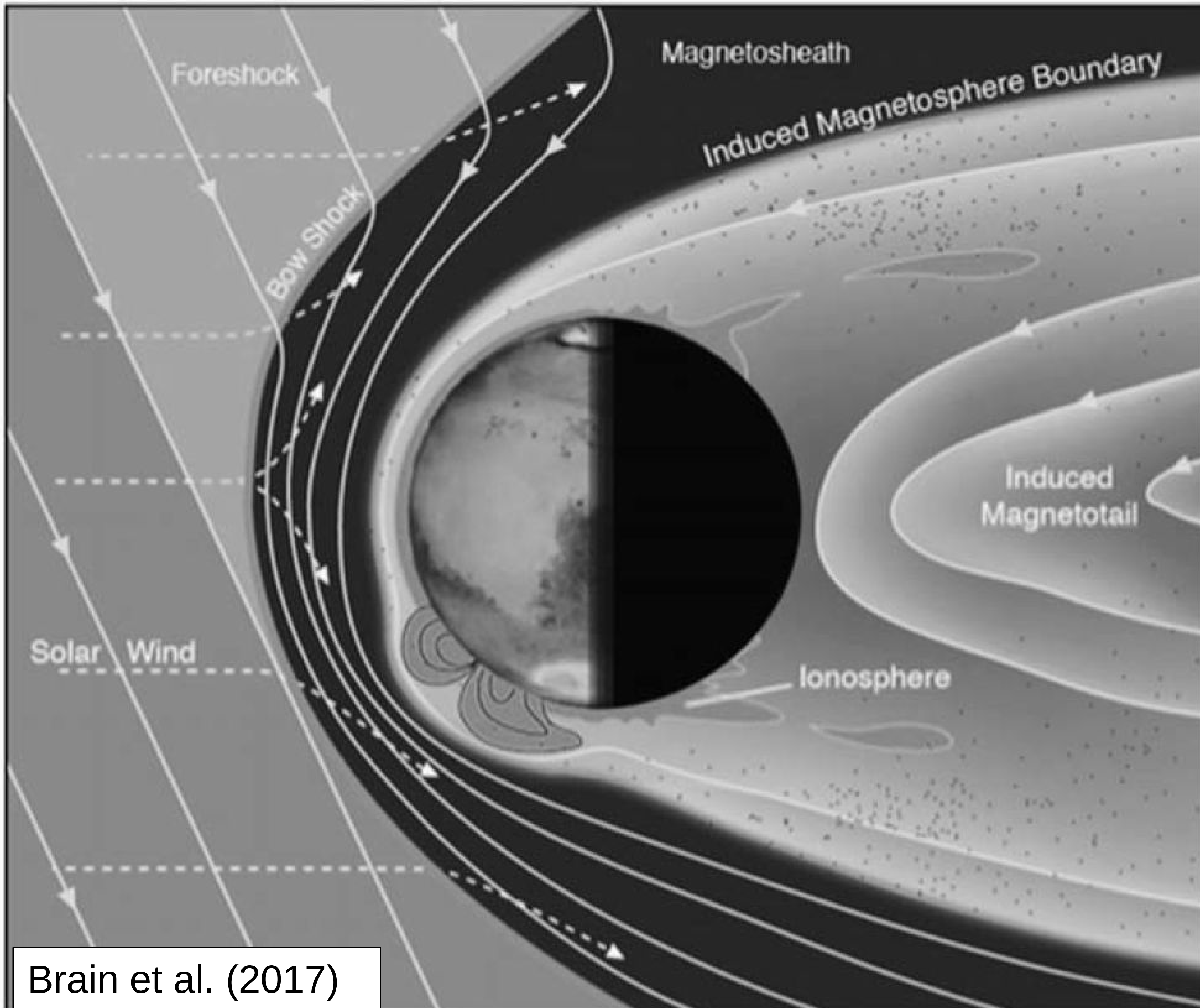

Brain et al. (2017)

MaRS radio science

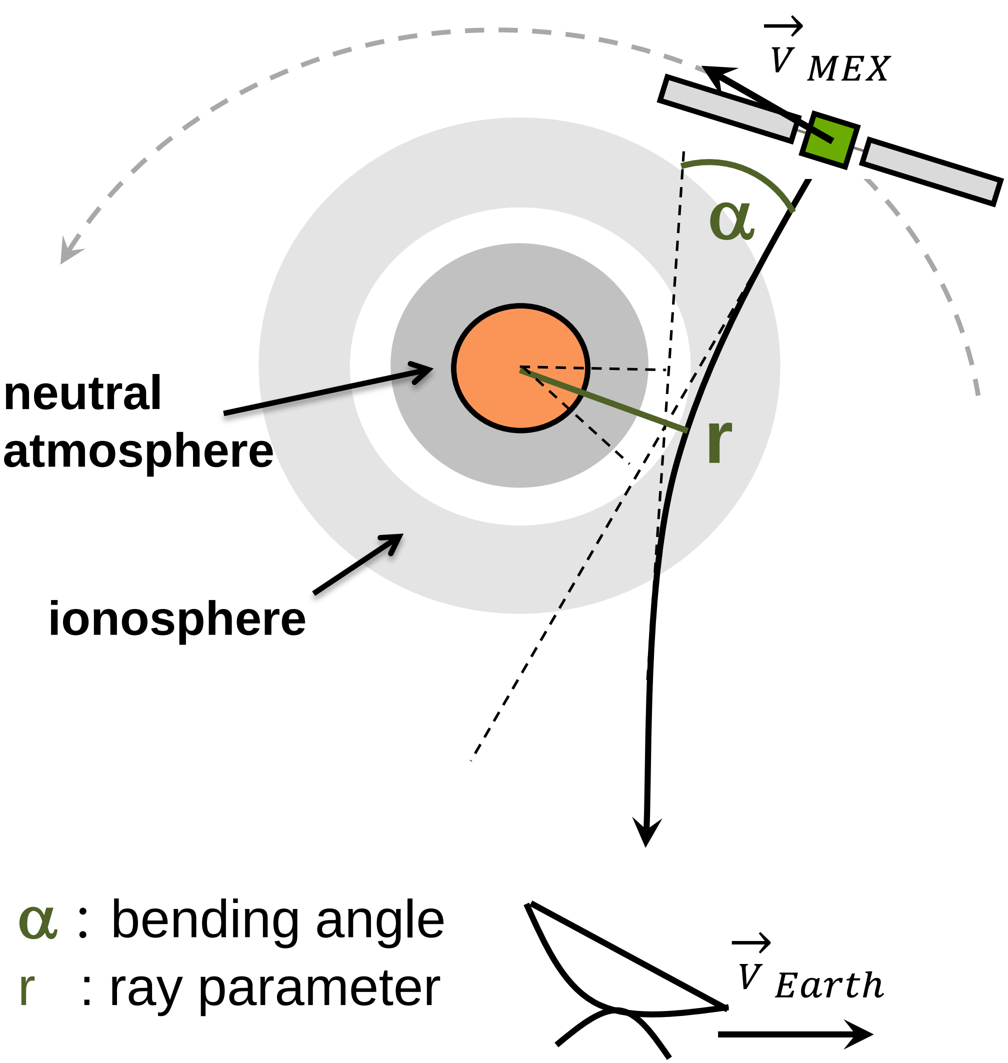

Figure adapted from S. Tellmann

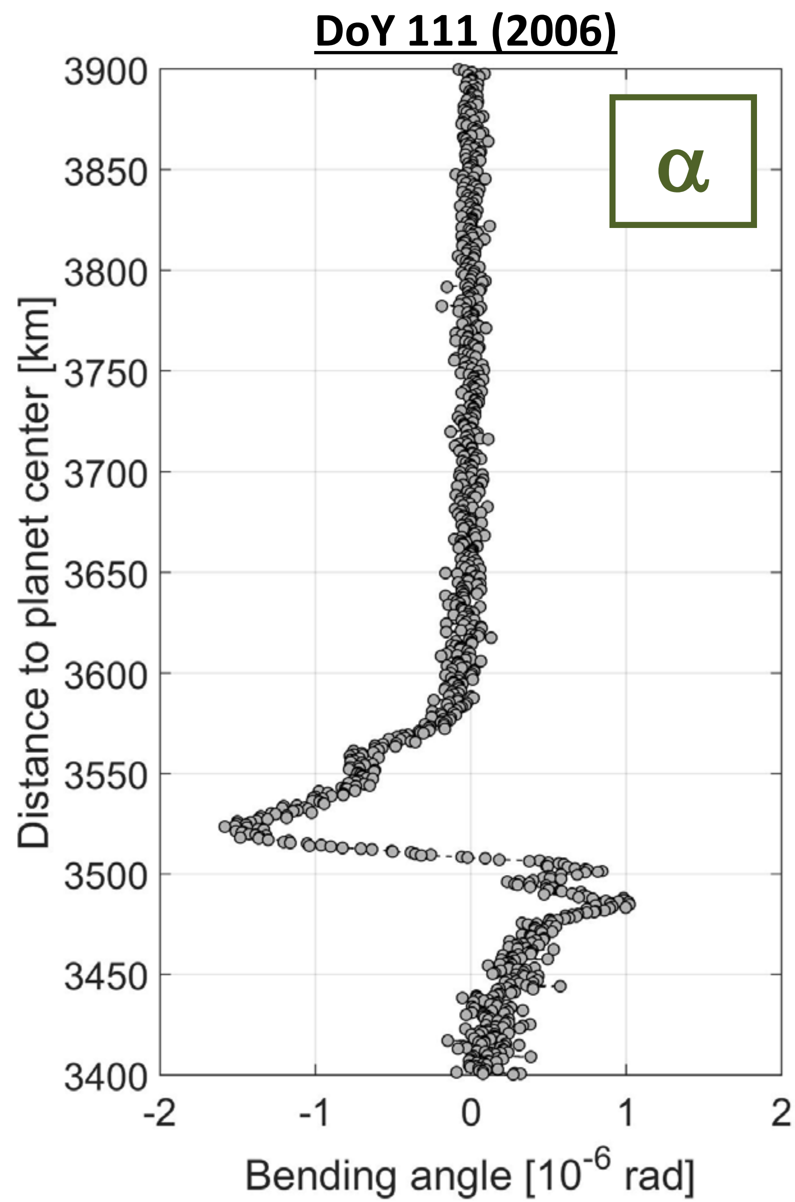

MaRS radio science

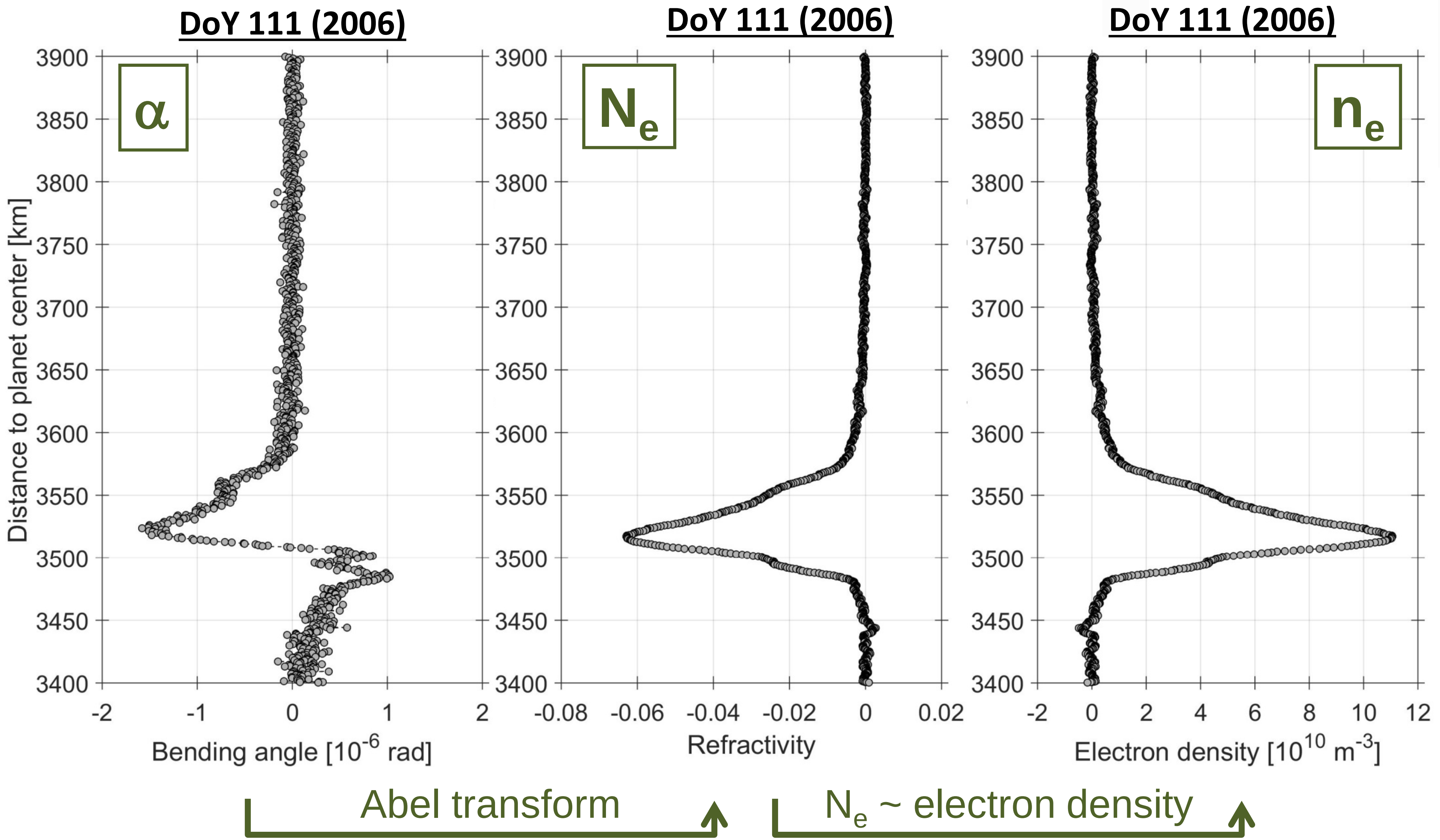

Observed are ionospheric electrons, not ions!

Mm: Sporadic E / crustal magnetic field

B_{tot} [nT] low	B_{tot} [nT] up	observations all [#]	observations Mm [#]	observations Mm [%]	B_{tot} [nT] low	B_{tot} [nT] up	observations all [#]	observations Mm [#]	observations Mm [%]
0	10	200	95	47.5	80	90	1	0	0.0
10	20	37	13	35.1	90	100	1	1	100.0
20	30	9	2	22.2	100	110	0	0	0.0
30	40	2	0	0.0	110	120	2	0	0.0
40	50	8	3	37.5	120	130	0	0	0.0
50	60	5	2	40.0	130	140	0	0	0.0
60	70	1	1	100.0	140	150	0	0	0.0
70	80	0	0	0.0	150	160	1	0	0.0

B_{tot} in 400 km altitude from MGS MAG/ER observations, *Connerney et al. 2001*

- MaRS data inconclusive concerning Mm occurrence rate dependence on high crustal magnetic fields
- Mm layers are available above regions with low crustal magnetic field

MaRS data sets

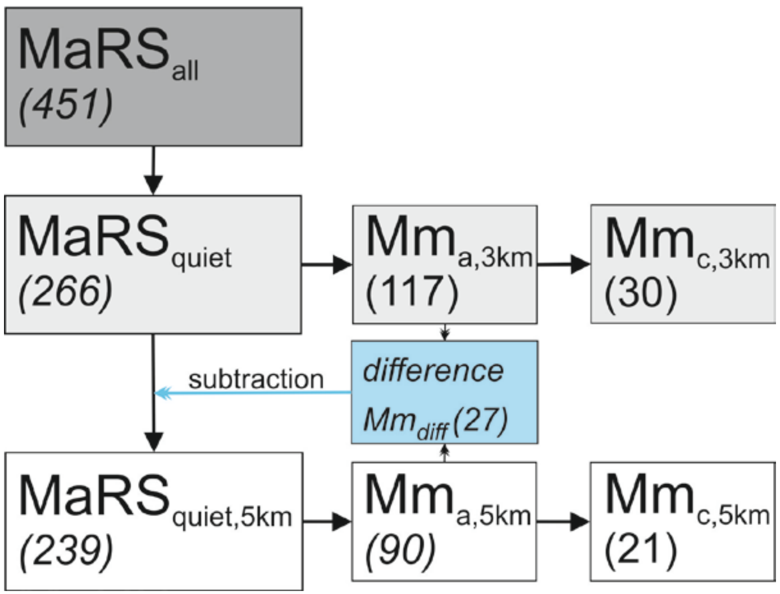

Mm$_{a,3km}$: all observations where

Mm TEC > 3000m◦3◦noise level

Mm$_{a,5km}$: all observations where

Mm TEC > 5000m◦3◦noise level

Mm$_{c,*}$: all observations where

- Lower baseline (LB) > 15 km
- Mm TEC > X m◦3◦noise level of the LB
- Mean offset < 6◦noise level of the LB

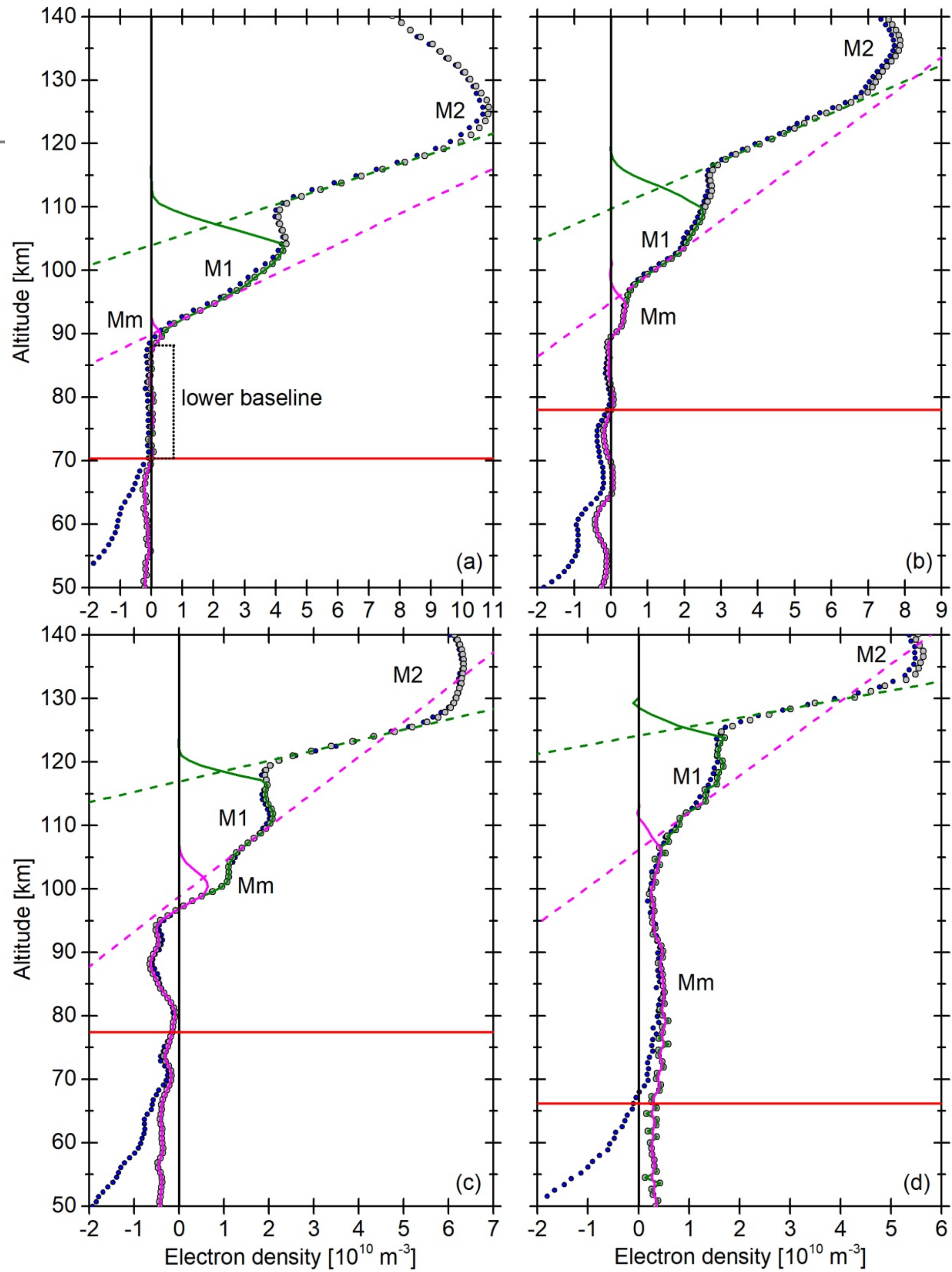

Mm: solar flux dependence

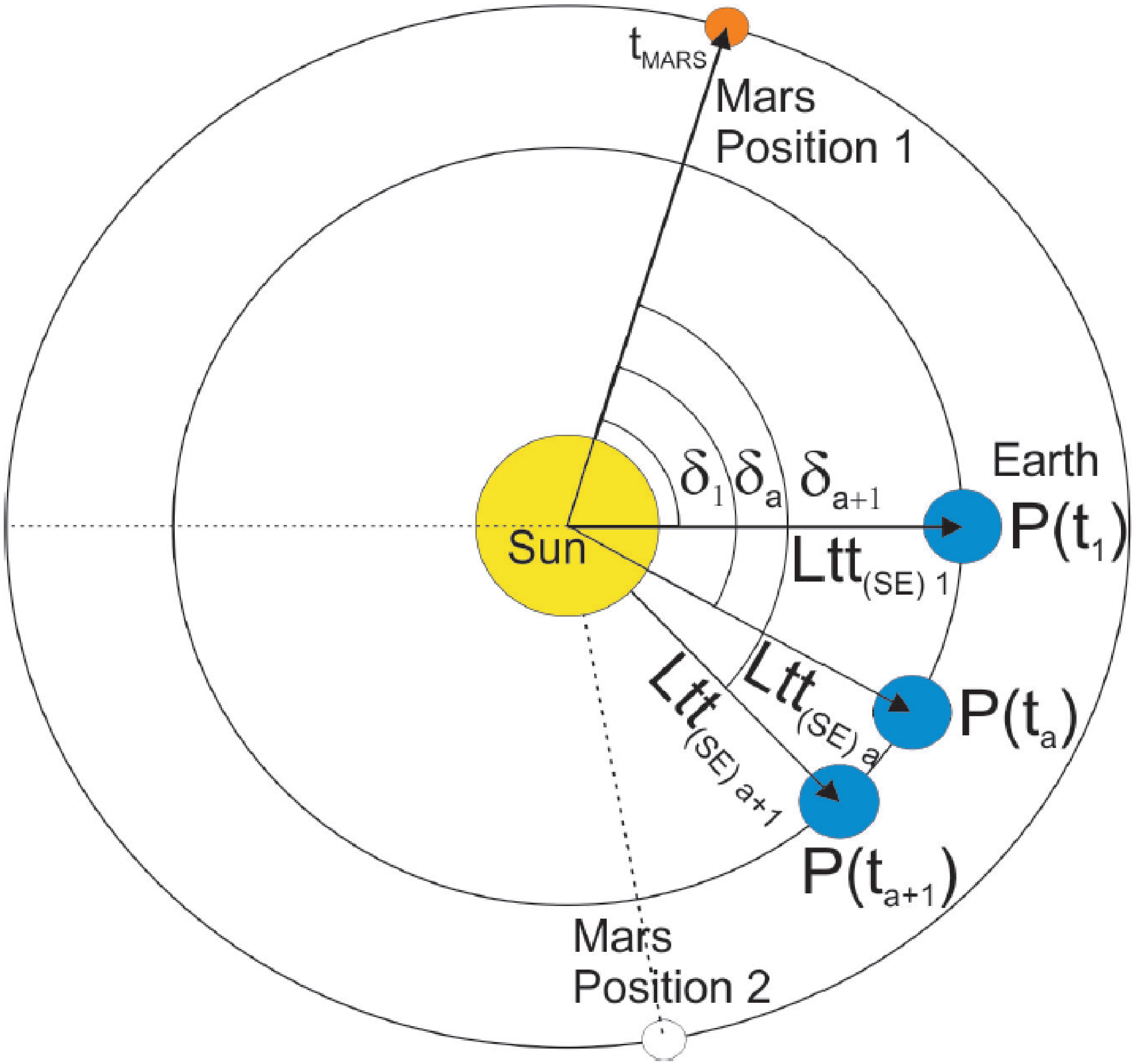

Mm: solar flux dependence

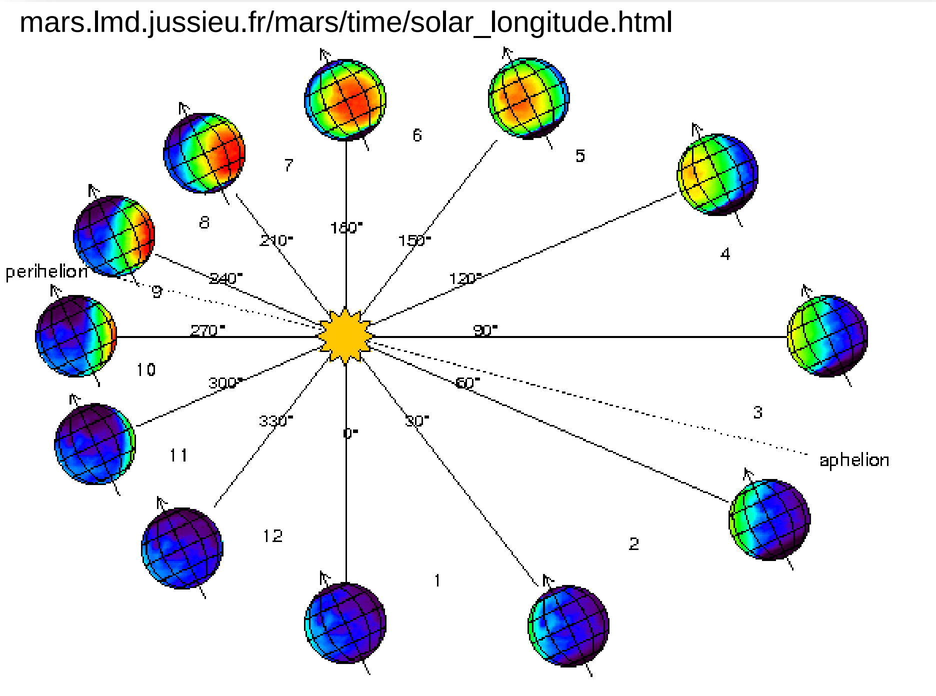

Solar flux parameters from

SIP V2.38 / Solar 2000,

1nm resolution, 1 data set/day

(Tobiska et al. 2000)

- Time and space calibration for the Mars position
  - Φ_{SUM} = **0.45 – 95 nm**
    full TEC + M2 el. density correlation
  - Φ_{Xray} = **0.45 – 10 nm**
    M1 TEC + M1 el. density correlation
  - $\Phi_{0.5\text{-}3.0}$ = **0.45 – 3 nm**
- Solar activity (no calibration)
  - Φ_{EARTH} = **0.45 – 95 nm**

Mm: solar flux dependence

	all [number]	$Mm_{a,3km}$ [number]	[%]
Φ_{SUM}			
low	39	15	**38.5**
moderate	189	90	**47.6**
high	38	12	**31.6**
Φ_{Xray}			
low	28	8	**28.6**
moderate	199	92	**46.2**
high	39	17	**43.6**
$\Phi_{0.45\text{-}3.0}$			
low	100	41	**41.0**
moderate	125	57	**45.6**
high	41	19	**46.3**
Φ_{EARTH}			
low	26	7	**26.9**
moderate	207	92	**44.4**
high	33	18	**54.5**

Solar flux parameters from SIP V2.38 / Solar 2000,

1nm resolution, 1 data set/day

(Tobiska et al. 2000)

- <u>Time and space calibration for the Mars position</u>
  - Φ_{SUM} = **0.45 – 95 nm**
    full TEC + M2 el. density correlation
  - Φ_{Xray} = **0.45 – 10 nm**
    M1 TEC + M1 el. density correlation
  - $\Phi_{0.5\text{-}3.0}$ = **0.45 – 3 nm**
- <u>Solar activity (no calibration)</u>
  - Φ_{EARTH} = **0.45 – 95 nm**

M2 vertical electron content

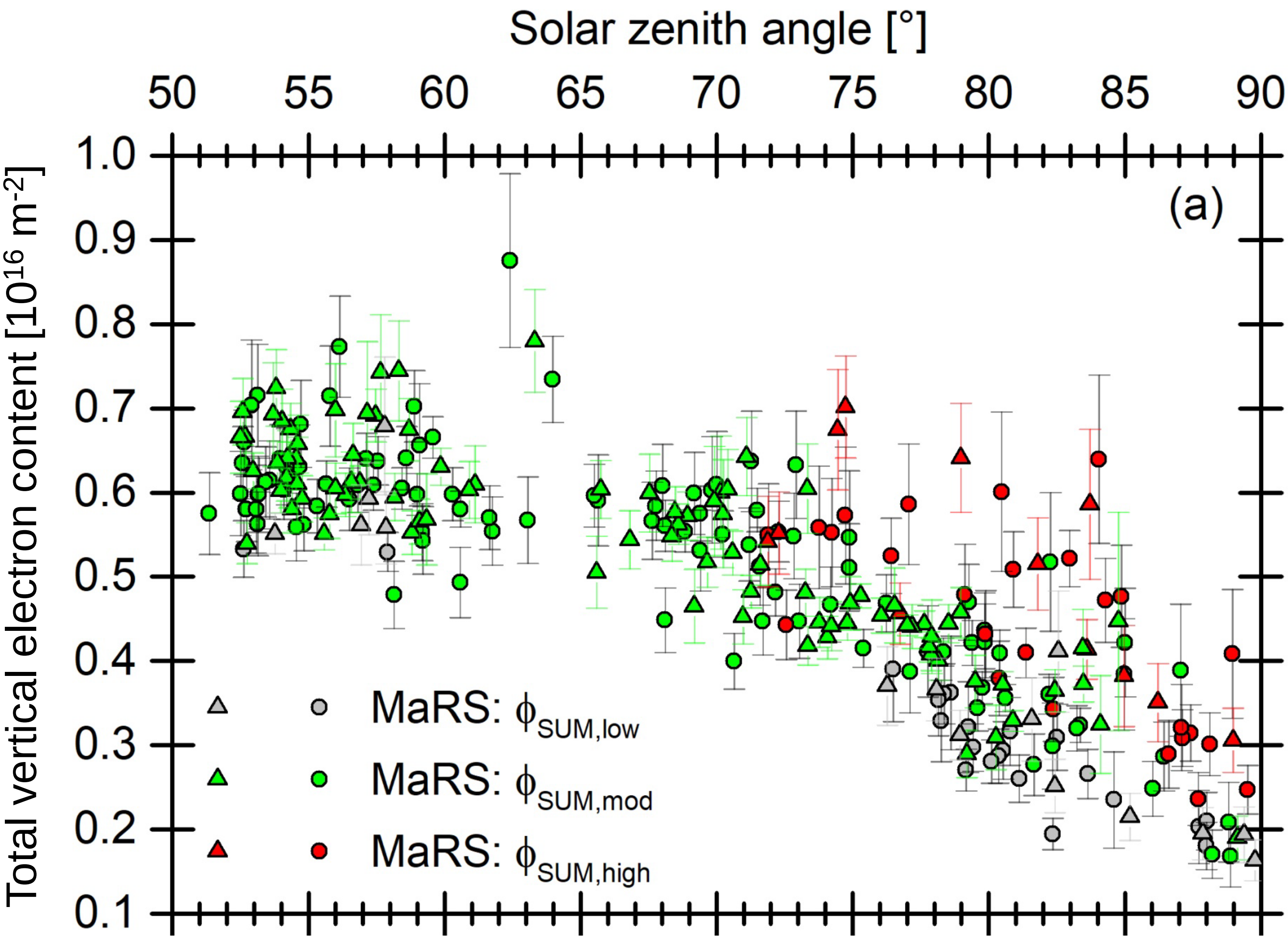

M2 electron density

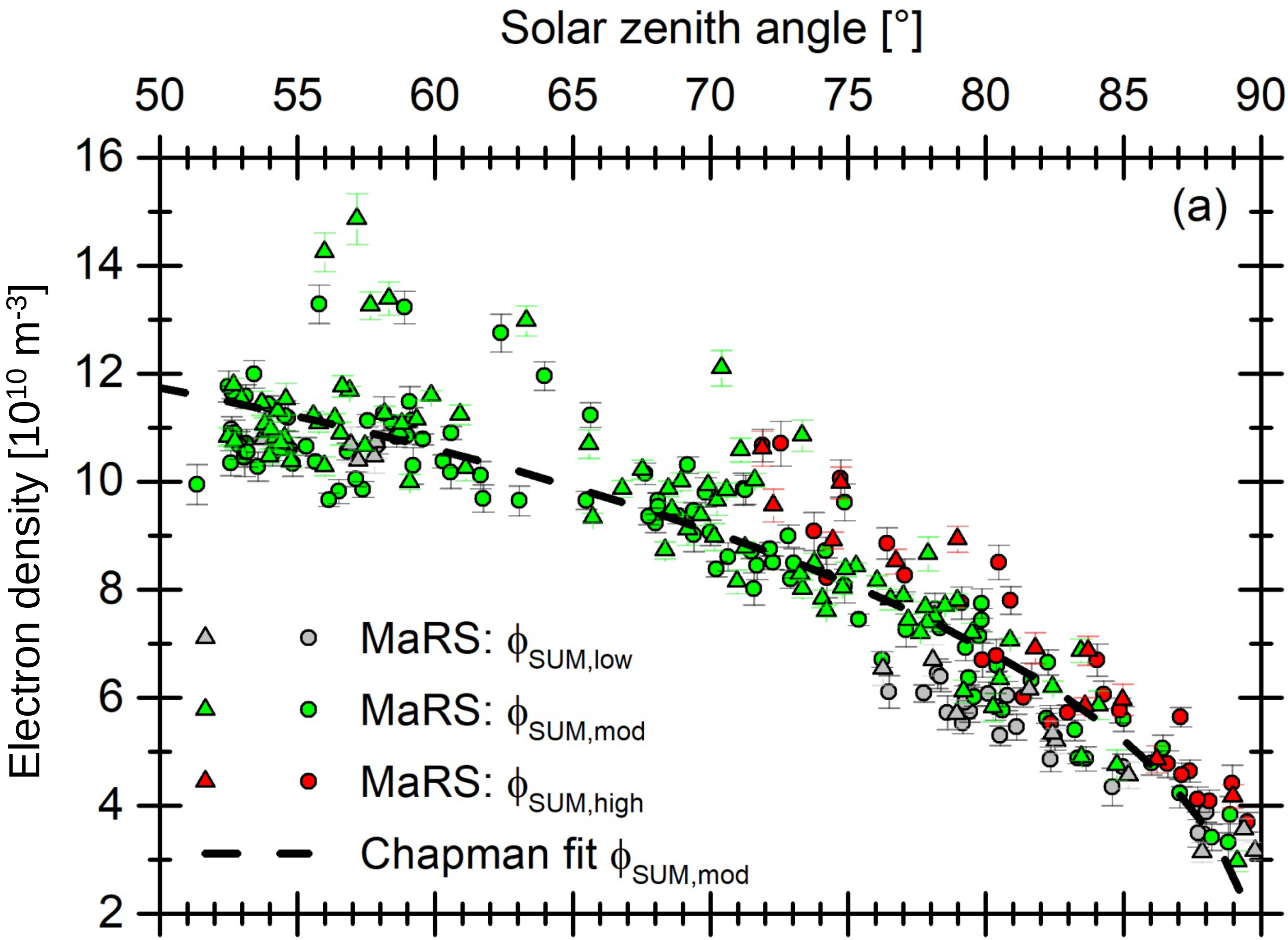

M2 altitude

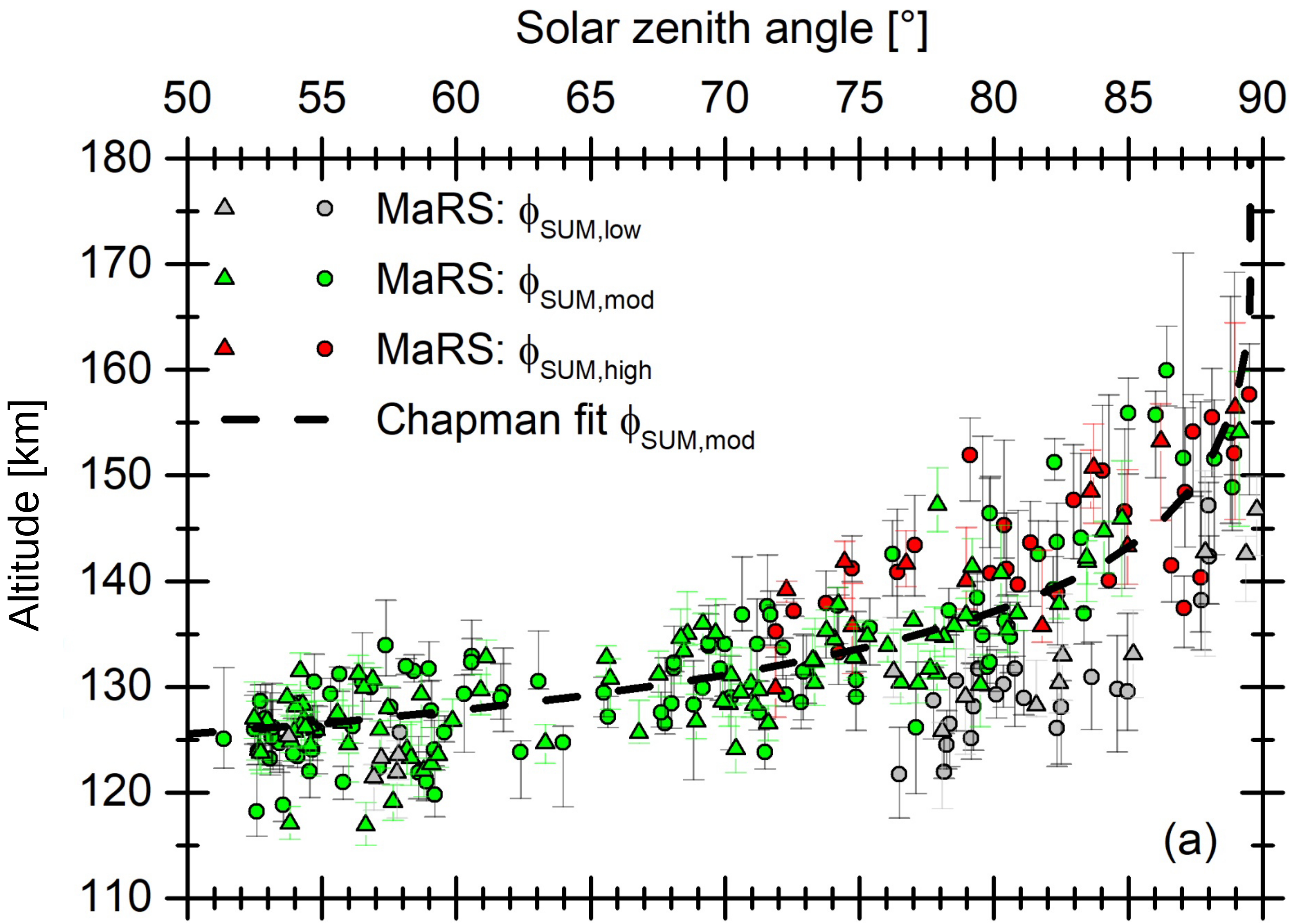

Solar zenith angle [°]
50
55
60
65
70
75
80
85
90
180
170
160
150
140
130
120
110
Altitude [km]
MaRS: $\phi_{SUM,low}$
MaRS: $\phi_{SUM,mod}$
MaRS: $\phi_{SUM,high}$
Chapman fit $\phi_{SUM,mod}$
(a)

M1 parameter derivation

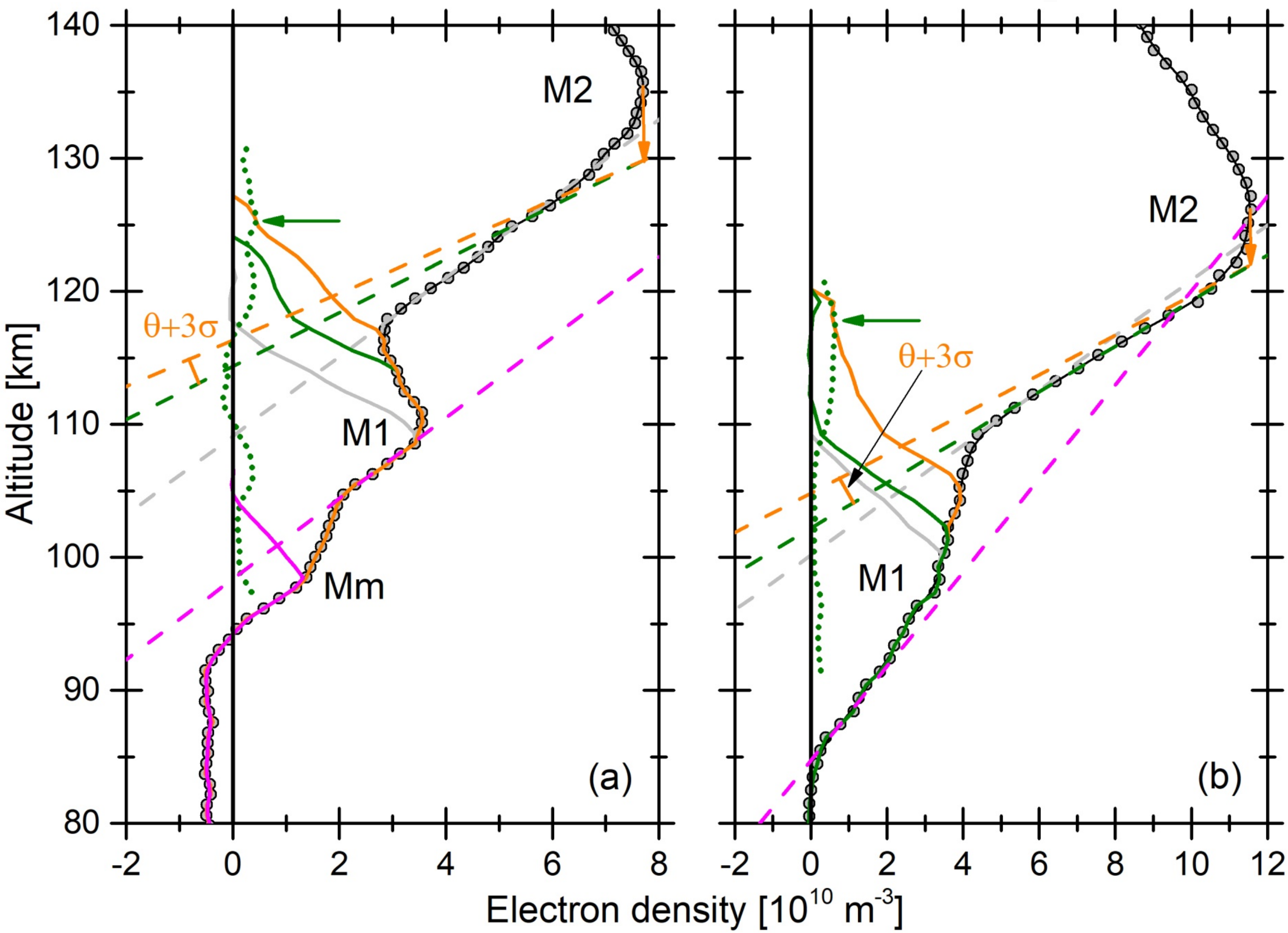

M1 vertical electron content

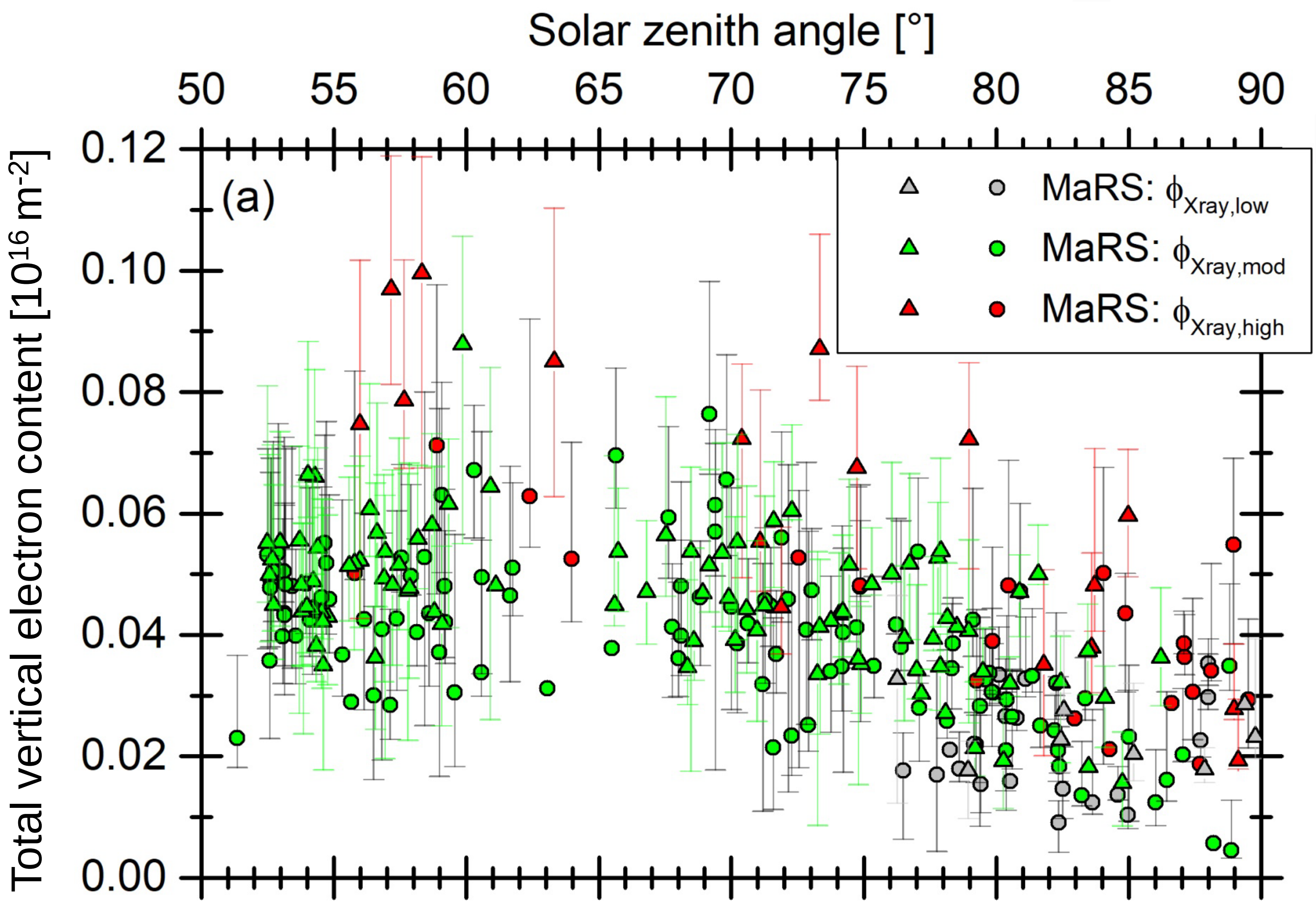

M1 electron density

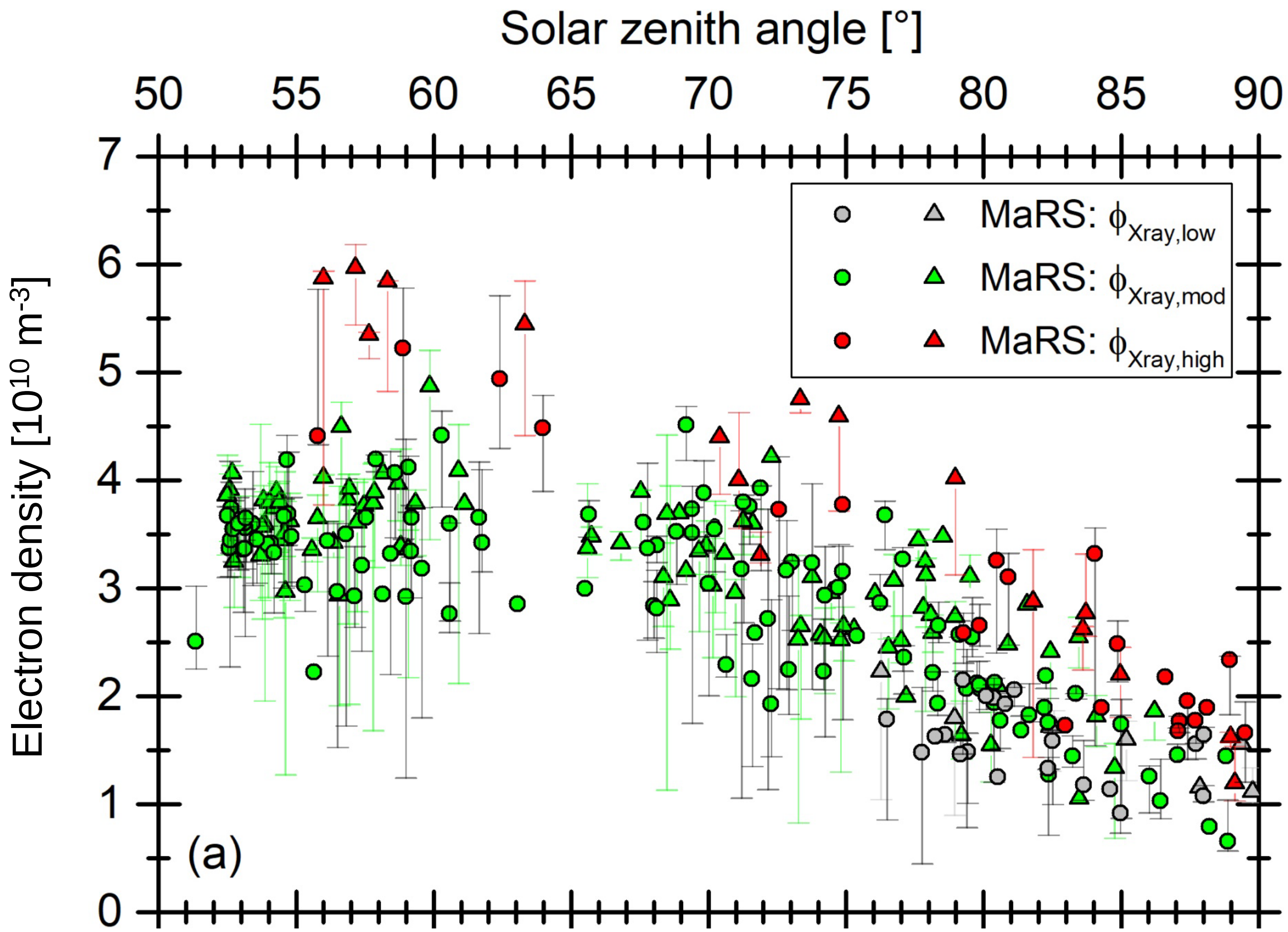

M1 altitude

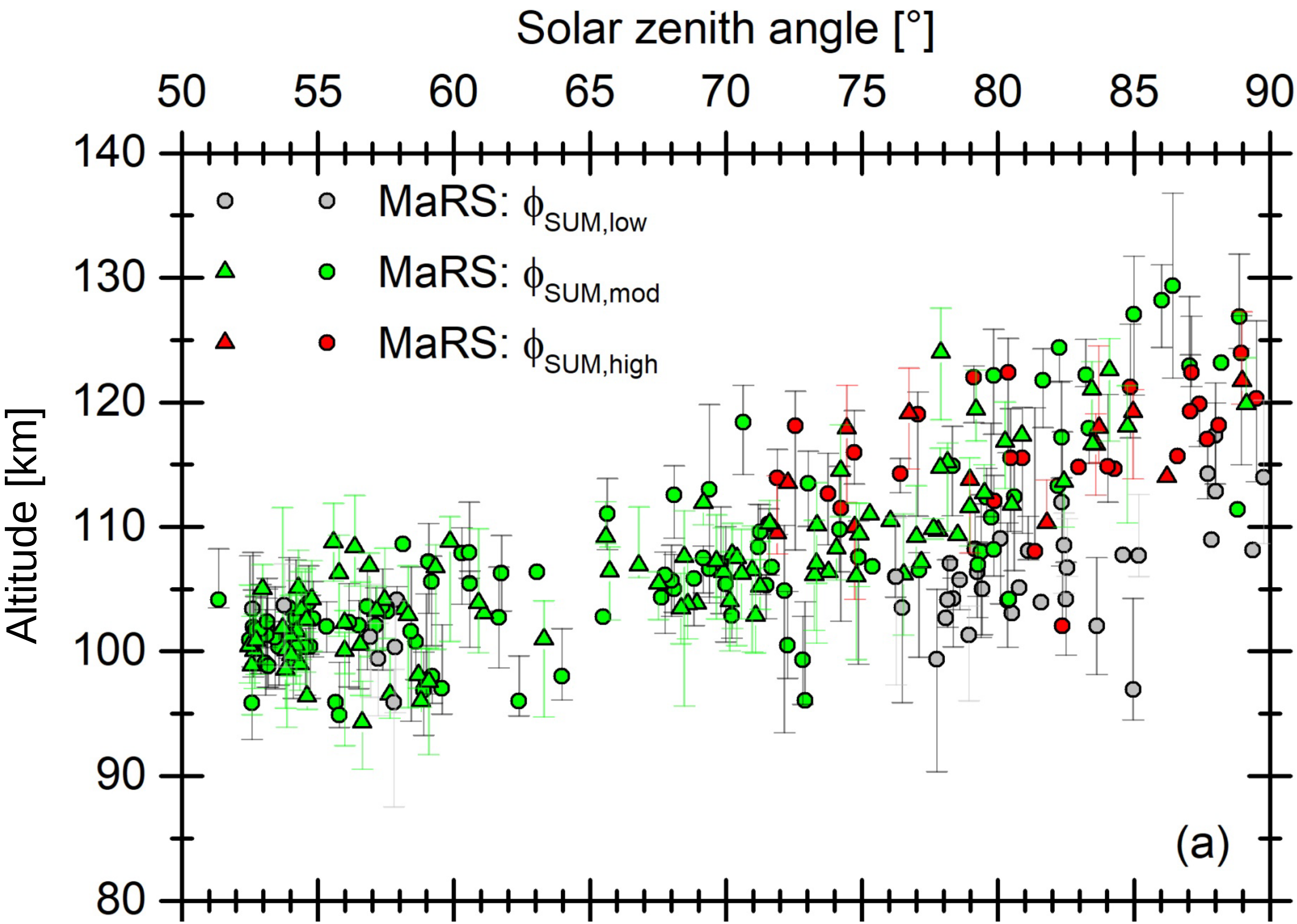

Solar zenith angle [°]
50
55
60
65
70
75
80
85
90
140
130
120
110
100
90
80
Altitude [km]
MaRS: $\phi_{SUM,low}$
MaRS: $\phi_{SUM,mod}$
MaRS: $\phi_{SUM,high}$
(a)

Mm: Local ions O_2^+ & NO^+

- Main production processes for NO^+ in the lower ionosphere are

$$O_2^+ + N \rightarrow NO^+ + O$$
$$O_2^+ + NO \rightarrow NO^+ + O_2$$

- NO^+ is assumed to be a terminal ion in the lower Mars ionosphere (several source reactions, but loss only by dissociative recombination).

- The balance between O_2^+ and NO^+ in the lower ionosphere depends on the local amount of N and NO.

IonA-2: Background

- Boltzmann equation

$$\frac{\partial f_s^B}{\partial t} + \boldsymbol{v}_s \cdot \nabla f_s + \boldsymbol{a}_s \cdot \nabla_v f_s = \frac{\delta f_s}{\delta t}$$

- 5-moment equations (momentum, continuity, energy)

- Diffusion transport from the momentum equation
  - $n_s w_s = -(K + D_s^m)\frac{\partial n_s}{\partial z} - n_s\left[K\left(\frac{<m>g}{k_B T_N} + \frac{1}{T_N}\frac{\partial T_N}{\partial z}\right) + D_s^m\left(\frac{m_s g}{k_B T_s} + \frac{1+\beta}{T_s}\frac{\partial T_s}{\partial z}\right)\right]$ (neutral)
  - $n_s w_s = -D_s^a\left[\frac{\partial n_s}{\partial z} + n_s\left(\frac{m_s g}{2k_B T_P} + \frac{1}{T_P}\frac{\partial T_P}{\partial z}\right)\right]$ (ambipolar)

- Temporal density change of the individual species from the continuity equation

$$\frac{\partial n_u}{\partial t} + \frac{\partial}{\partial z}(n_u w_u) = P_u^{tot} - L_u^{tot}$$

IonA-2 solar flux 0.5 – 800 nm

DoY 336, 2005
78°

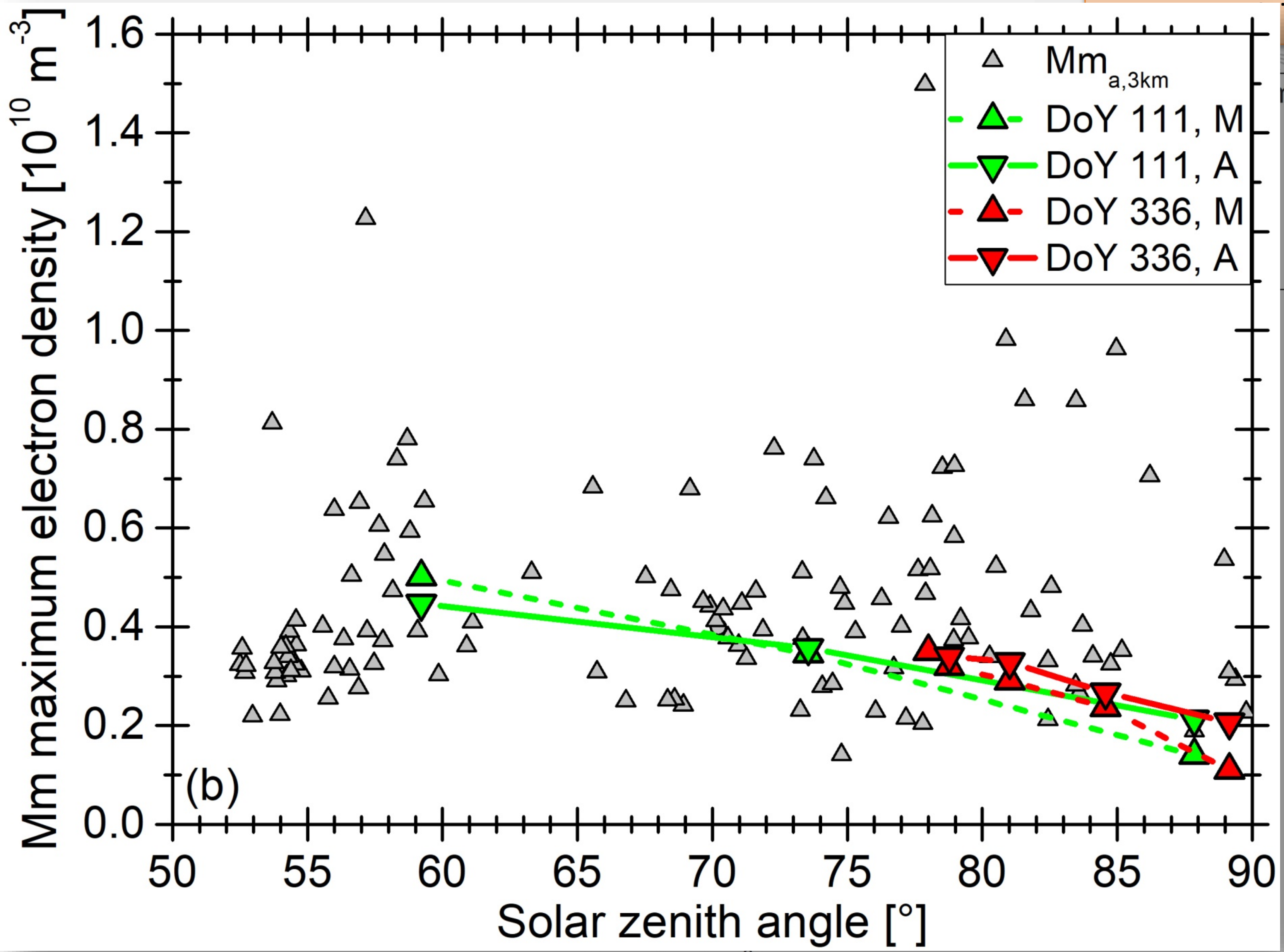

Density [m^{-3}]

IonA-2 solar flux 0.5 – 800 nm

DoY 336, 2005

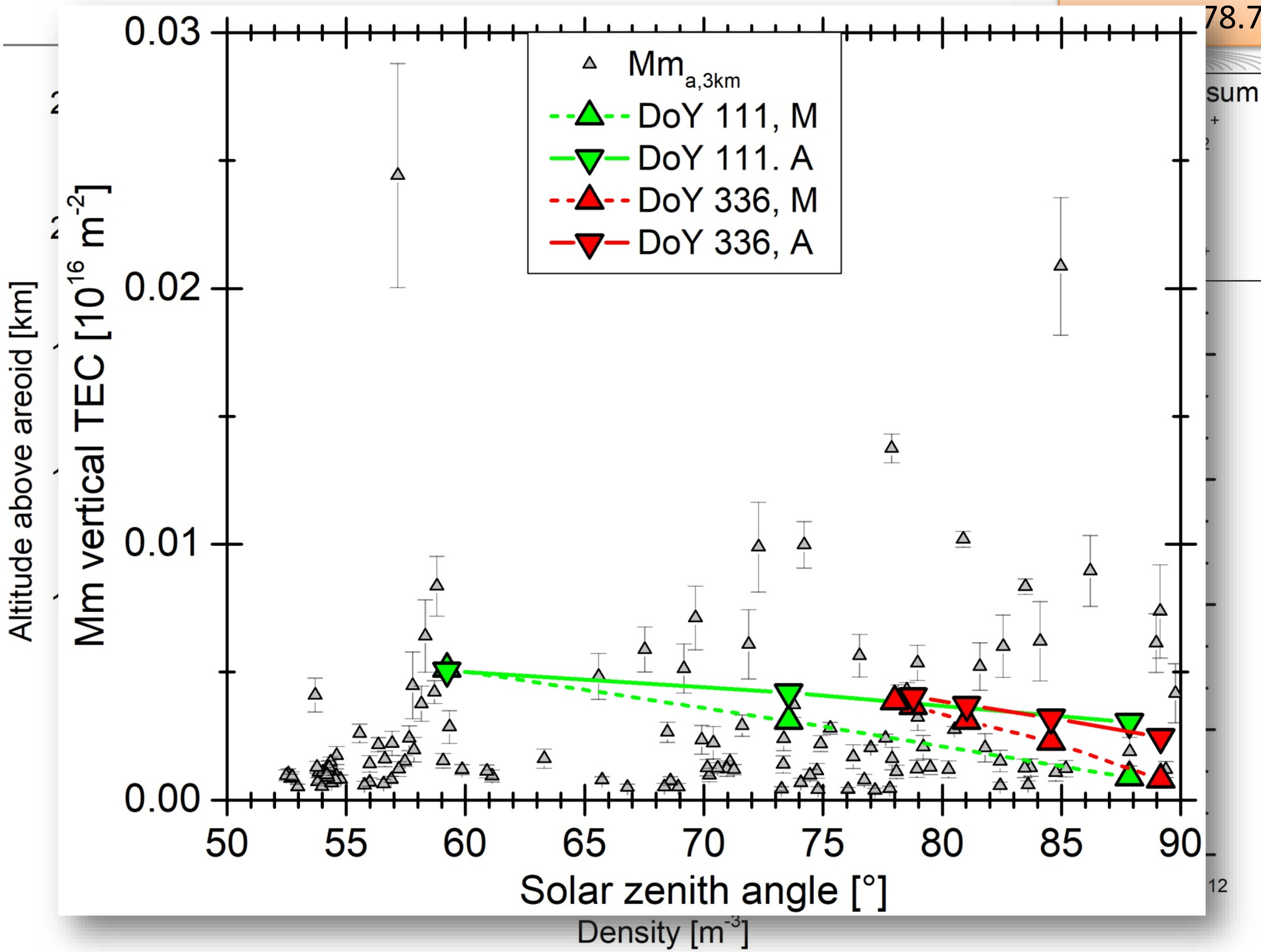

IonA-2 solar flux 0.5 – 800 nm

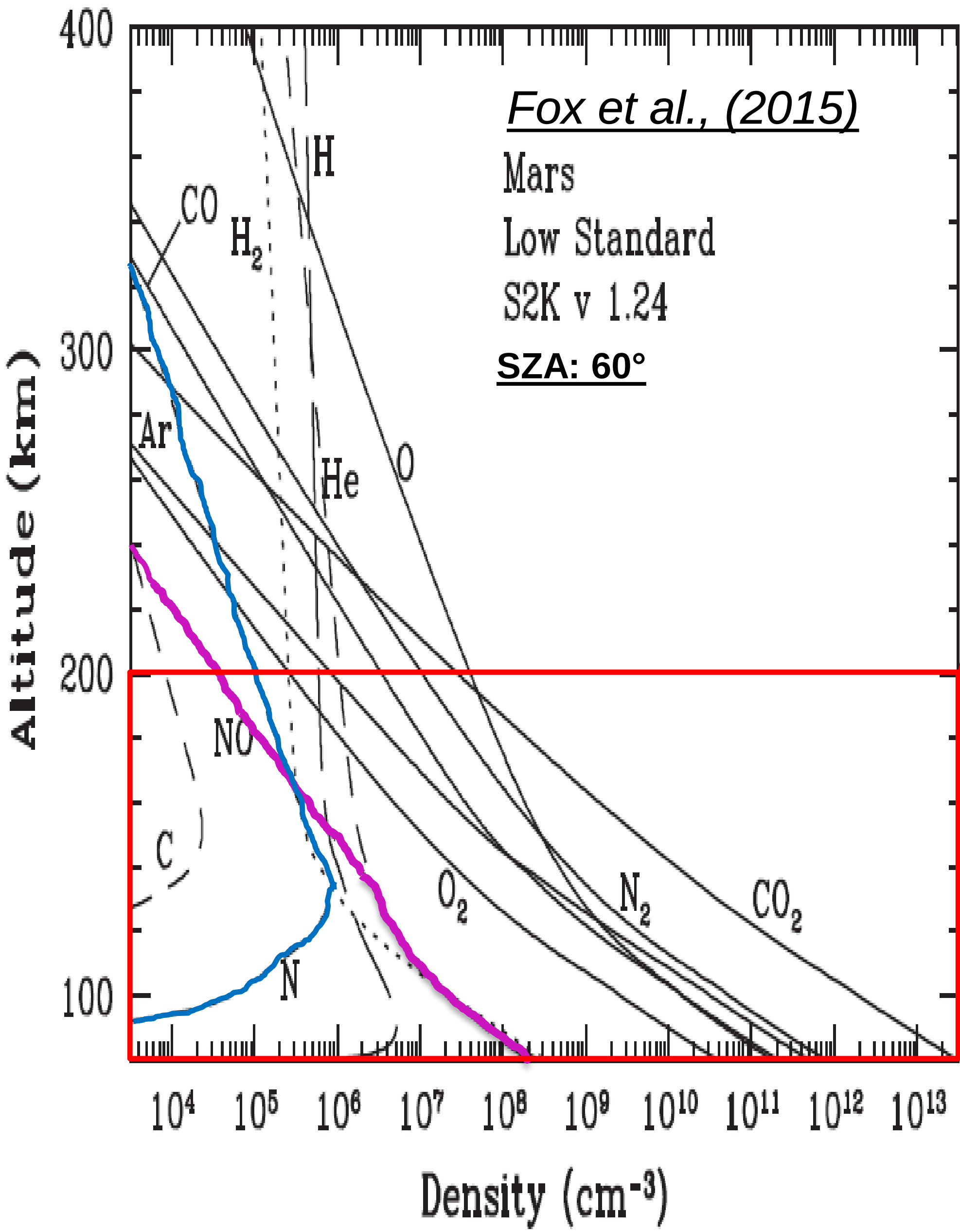

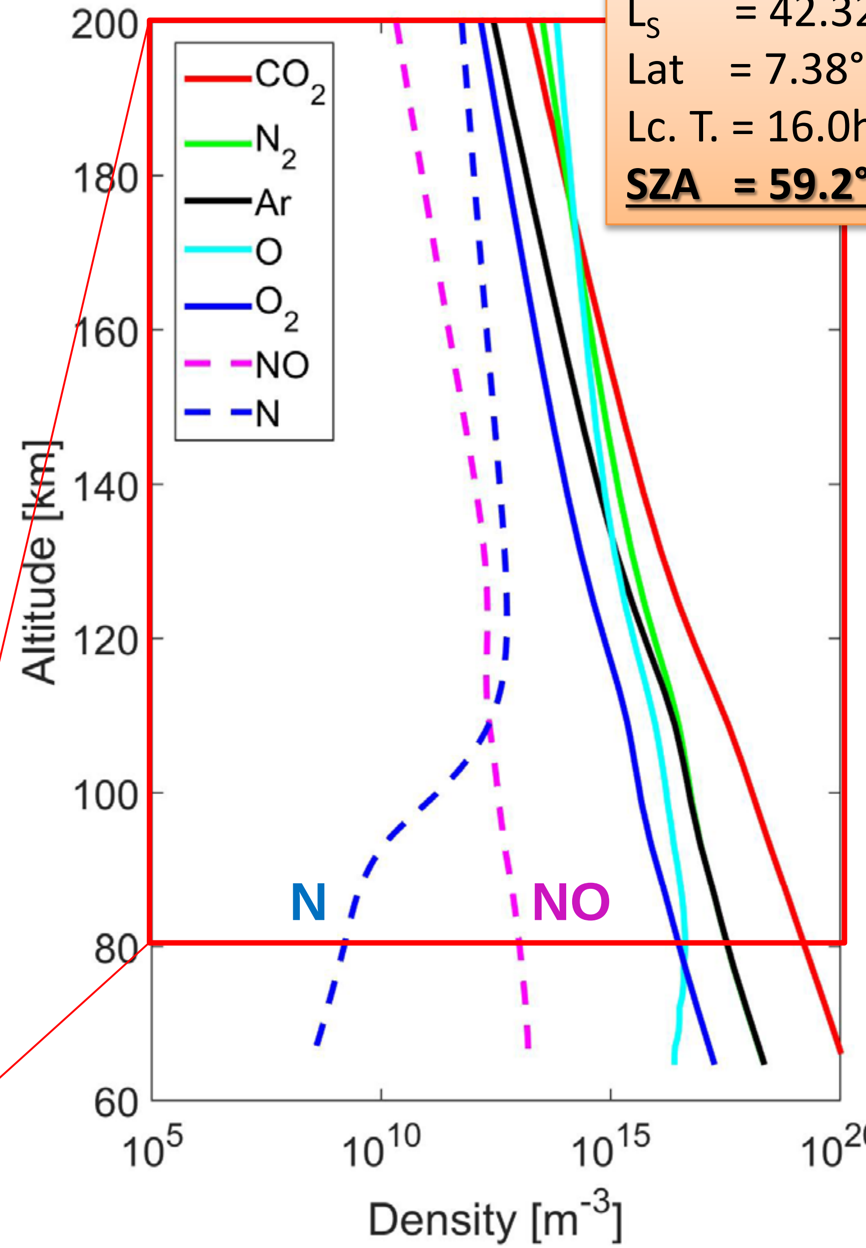

DoY 111, 2006
L_S = 42.32°
Lat = 7.38°
Lc. T. = 16.0h
SZA = 59.2°

32 Sol + 7 Mars hrs model run time

General agreement with *Fox et al., (2015)*

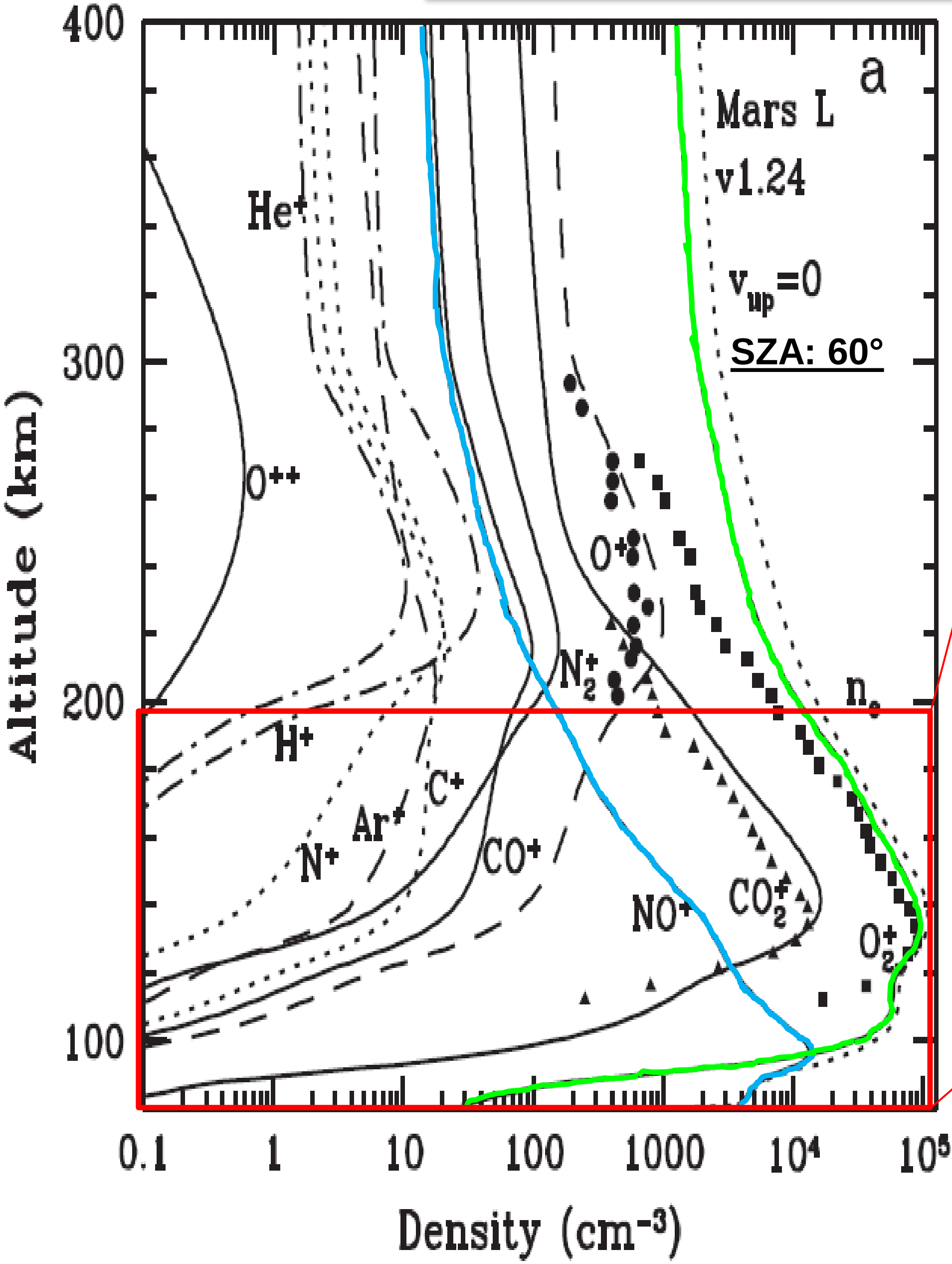

Fox et al., (2015)

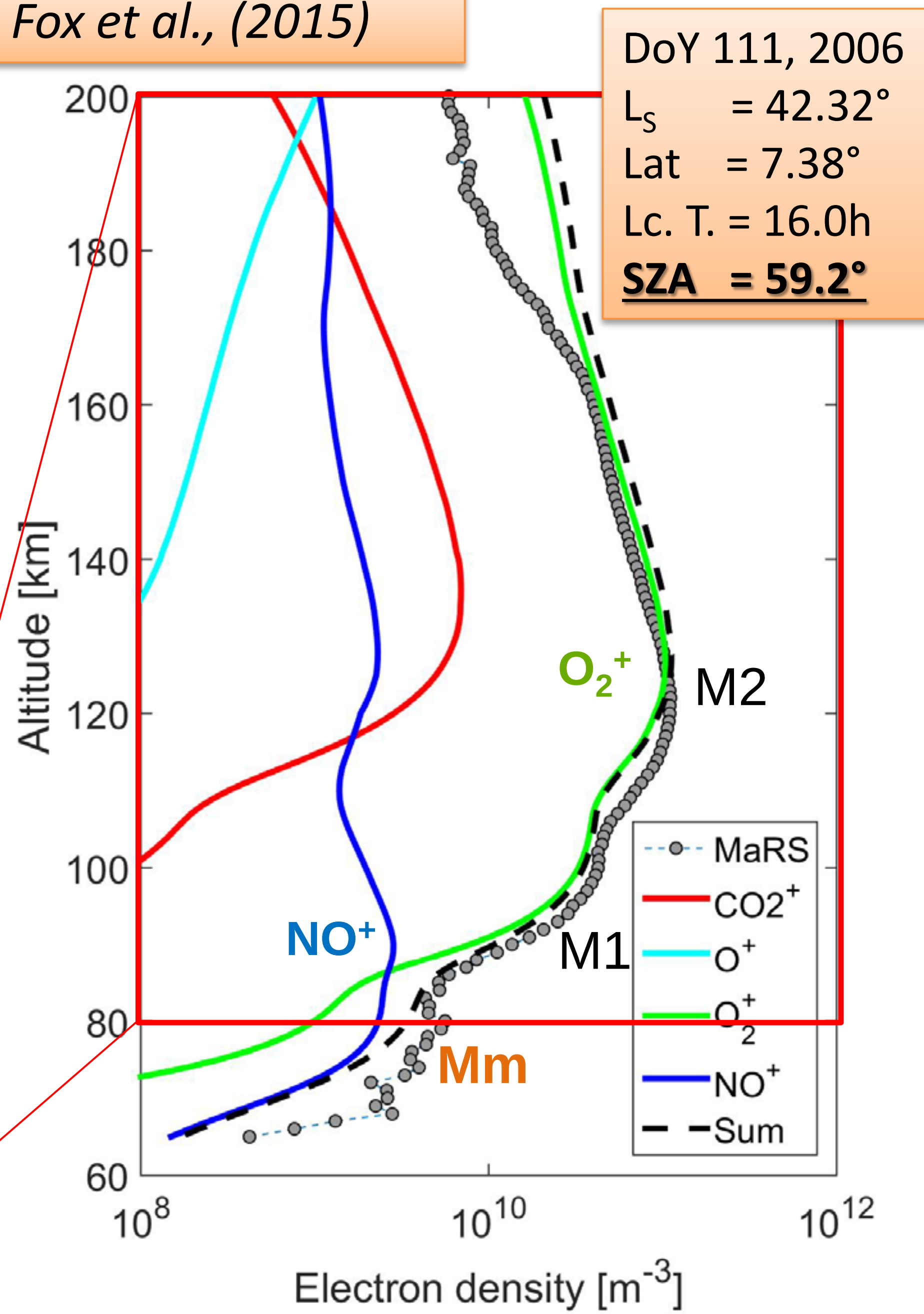

32 Sol + 7 Mars hrs model run time

Viking & MAVEN: electron temperature

- Viking lander in-situ observations
  - 20 July 1976 (23°N, L_S=97°, LST=16:13)
  - 3 September 1976 (48°N, L_S=118°, LST=9:49)
  - Start of northern summer, near aphelion, SZA ~ 45°
  - Solar minimum conditions (F10.7 ~ 70 at Earth)

- MAVEN deep dip September 2015 (*Vogt et al., 2017*)
  - 37 consecutive orbits from September 2. to September 9.
  - Lowering MAVEN periapsis below ionospheric peak for the first time on the planetary dayside
    - below 123 km altitude
    - Solar zenith angle 79° to 86° at main peak
  - Decreasing solar cycle (F10.7 ~ 88 at Earth)

Viking & MAVEN: electron temperature

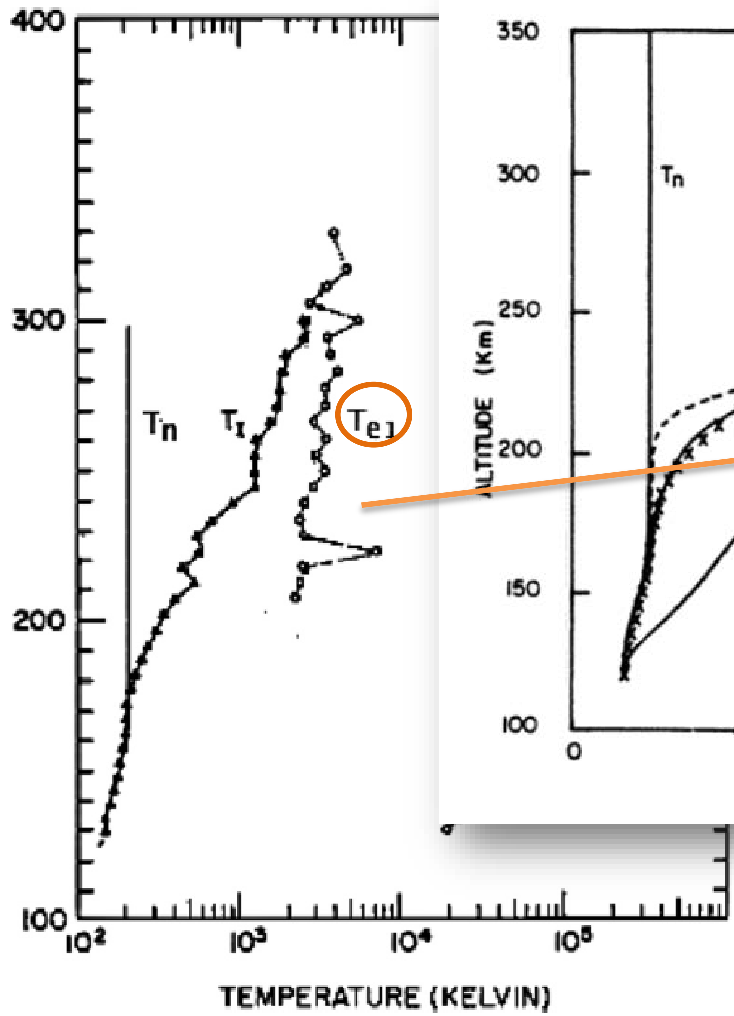

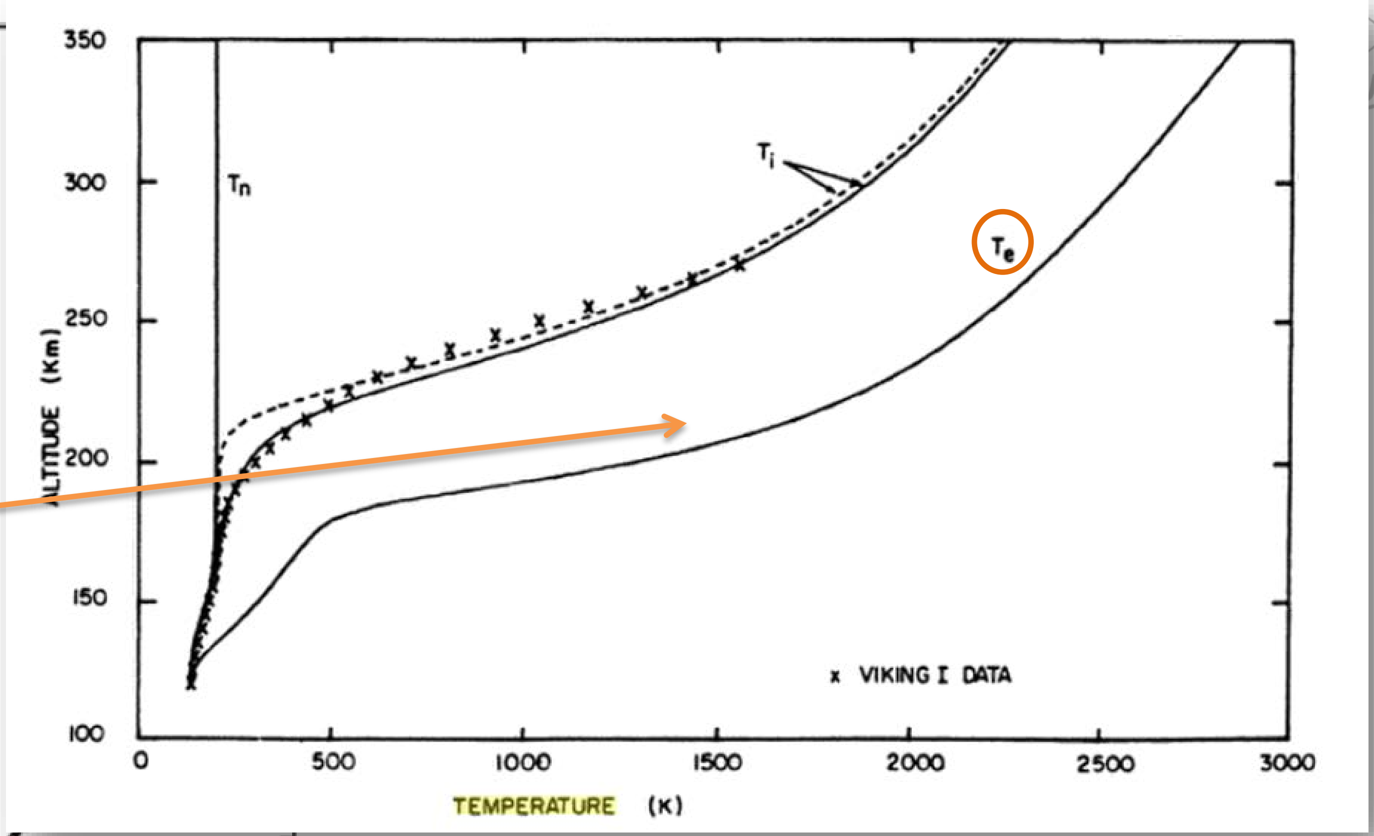

Viking lander in-situ temperatures
Hanson and Mantas, (1977)

Electron temperature derived by
Rohrbaugh et al., (1979)
from Viking observations
Used in IonA-2

Viking & MAVEN: electron temperature

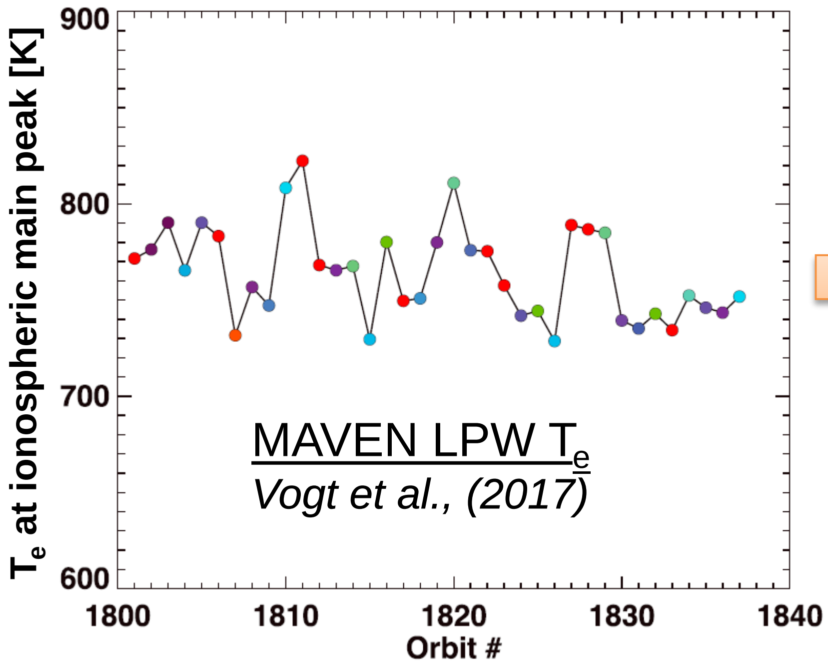

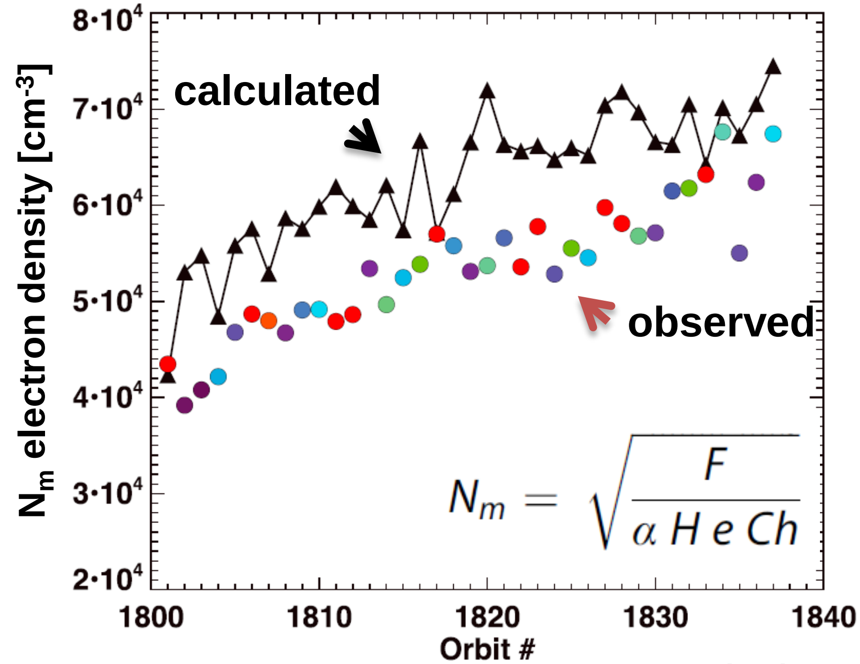

Vogt et al., (2017)

- MAVEN-LPW T_e at ionospheric peak altitude much higher than in Viking observations
- Electron density equilibrium calculation of *Vogt et al., (2017)* without secondary ionization exceeds observed LPW main peak electron densities.

- F: ionizing flux $9\cdot10^{-4}$ W/m^2
- α: O_2^+ diss. rec. coeff.
- H: scale height 10 km
- Ch: Chapman function for grazing incidence angle
- e: base of the natural logarithm
- N_m: calculated equilibrium electron density

Open questions: electron temperature

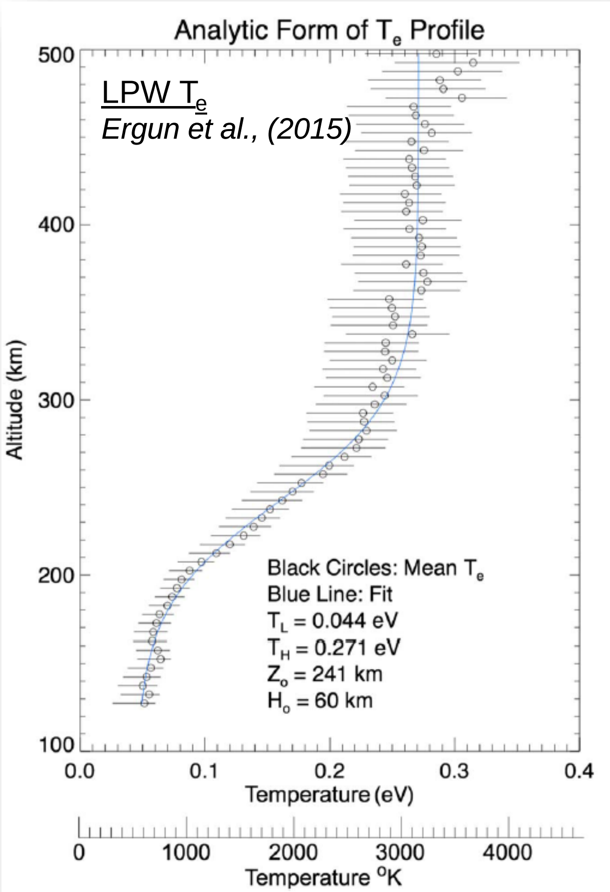

- T_e overestimate at low altitudes possible
  Ergun et al., (2015)
- *Derivation of IonA-2 T_e by interpolation between MCD neutral temperature T_n at 120 and LPW T_e at 130 km.*

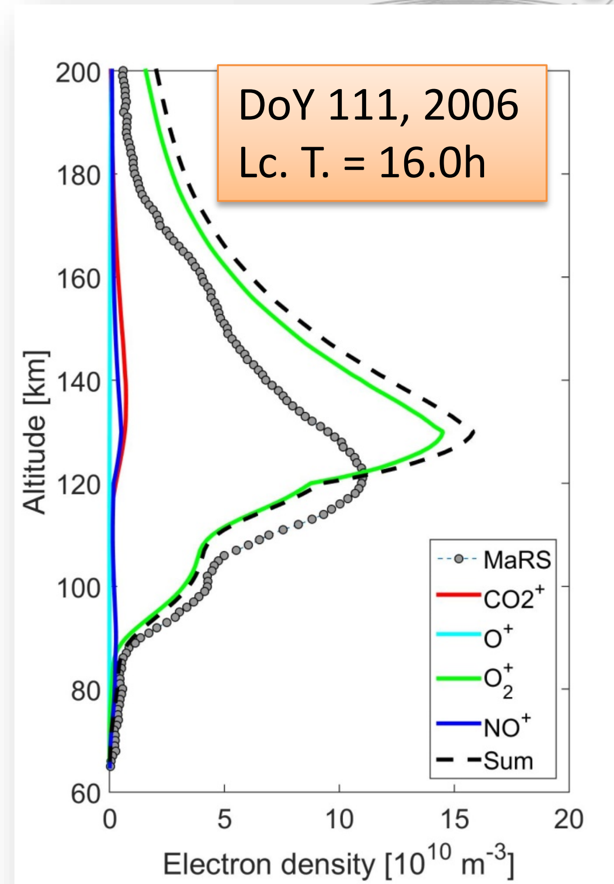

- MAVEN-LPW T_e at ionospheric peak altitude >> Viking observations
- Electron density equilibrium calculation of *Vogt et al., (2017)* from LPW T_e without secondary ionization exceeds observed LPW main peak electron densities.
- **Using the new MAVEN-LPW T_e in IonA-2 causes a large overestimation of the main peak electron density.**

Open questions: MAVEN NGIMS N density

NGIMS Averaged data for SZA 45°

Mahaffy et al., (2015)

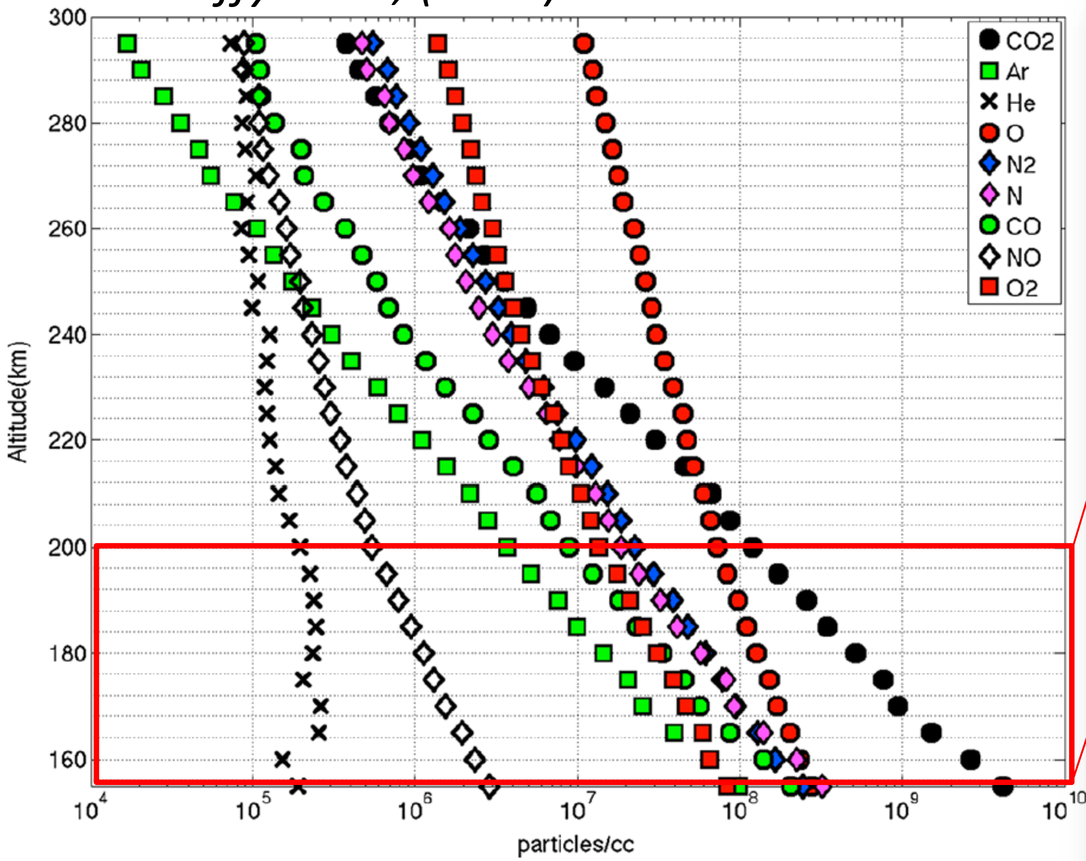

IonA-2
DoY 111, 2006
SZA = 59.2°

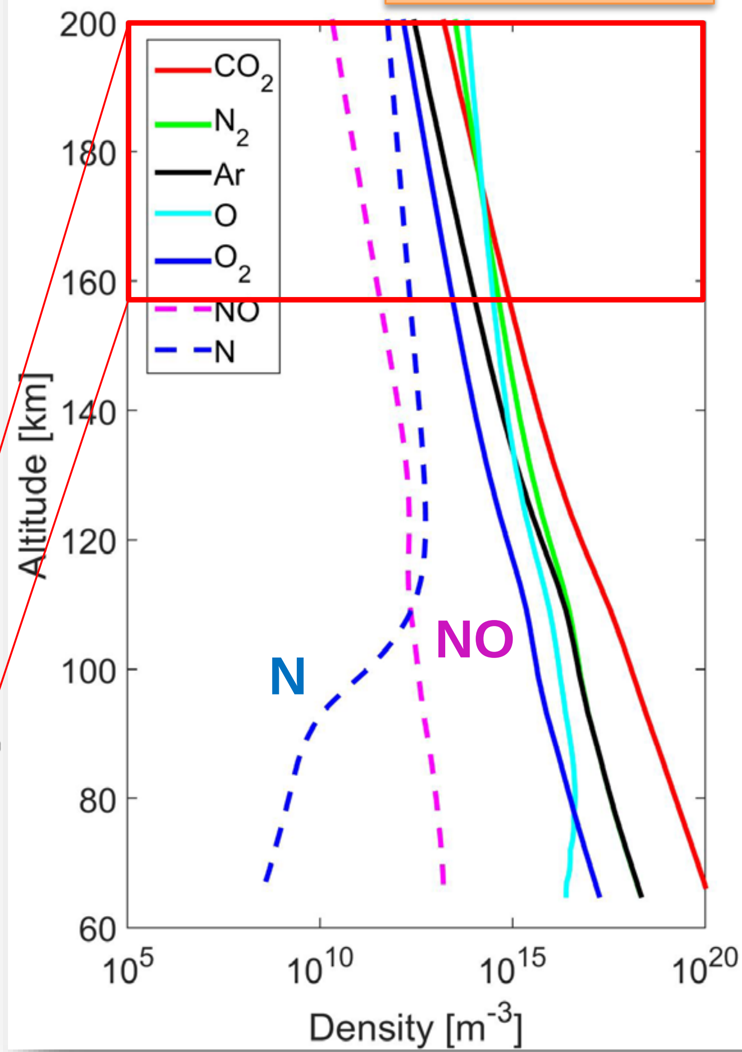

Large difference between IonA-2 modeled and observed NGIMS N densities.

Open questions: MAVEN NGIMS N density

•

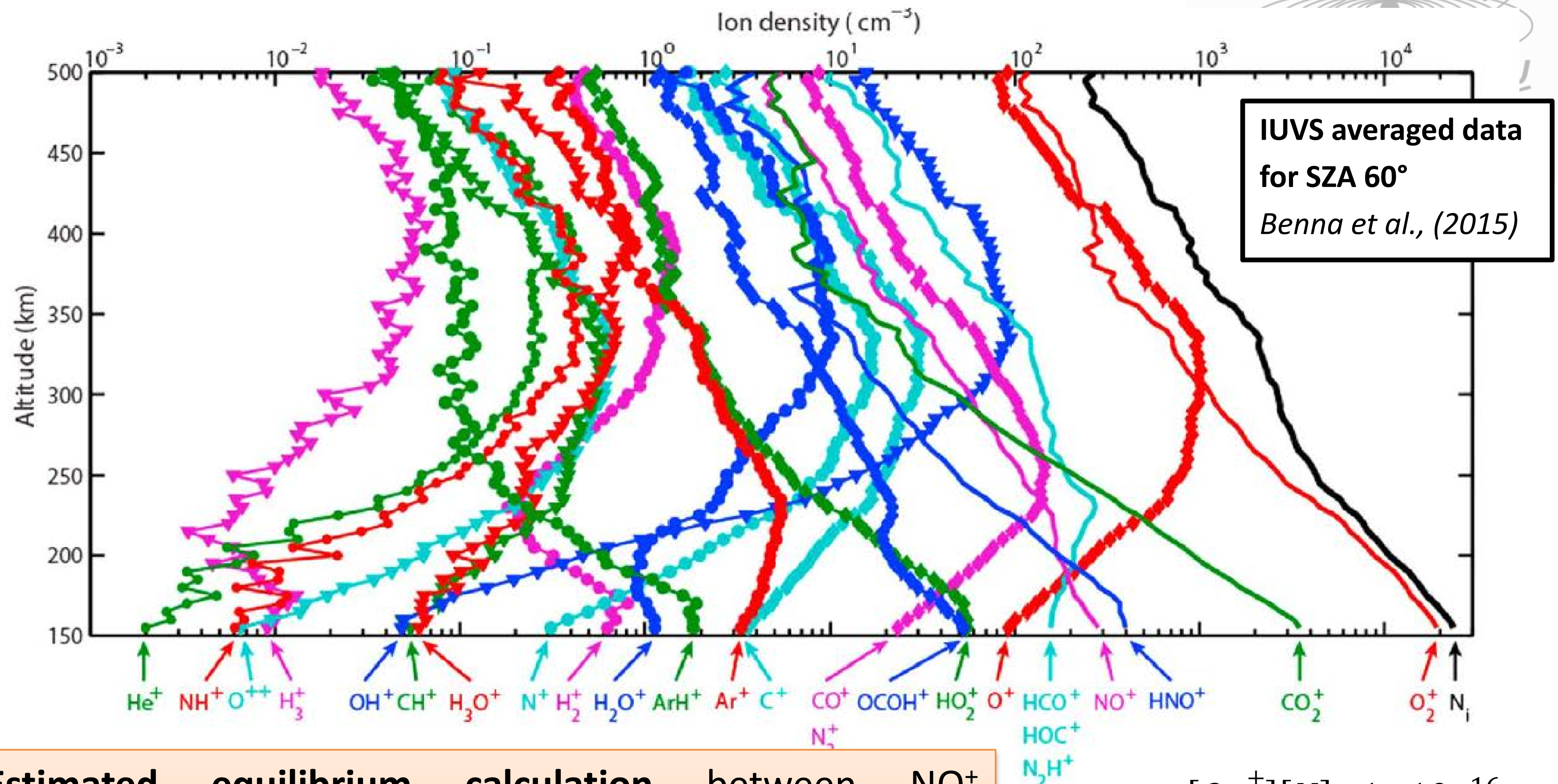

- **Estimated equilibrium calculation** between NO^+ production by reaction of N with O_2^+ and loss by dissociative recombination yield
  NO^+(155 km) ~ $1.8 \cdot 10^{12}$ m^{-3}
- **IUVS observation** provide approx.
  NO^+(155 km) ~ $3 \cdot 10^{8}$ m^{-3}!

$$NO^+ = \frac{[O_2{}^+][N] \cdot 1 \cdot 10^{-16}}{[n_e] \cdot 2 \cdot 10^{-14} \left(\frac{300\ K}{T_e}\right)^{0.8}}$$

O_2^+ ~ $2 \cdot 10^{10}$ m^{-3} (IUVS)
N ~ $2 \cdot 10^{14}$ m^{-3} (NGIMS)
n_e ~ $2.5 \cdot 10^{10}$ m^{-3} (IUVS)
Te ~ 800 K (LPW)

MAVEN NGIMS N density

NGIMS Averaged data for SZA 45° *Mahaffy et al., (2015)*

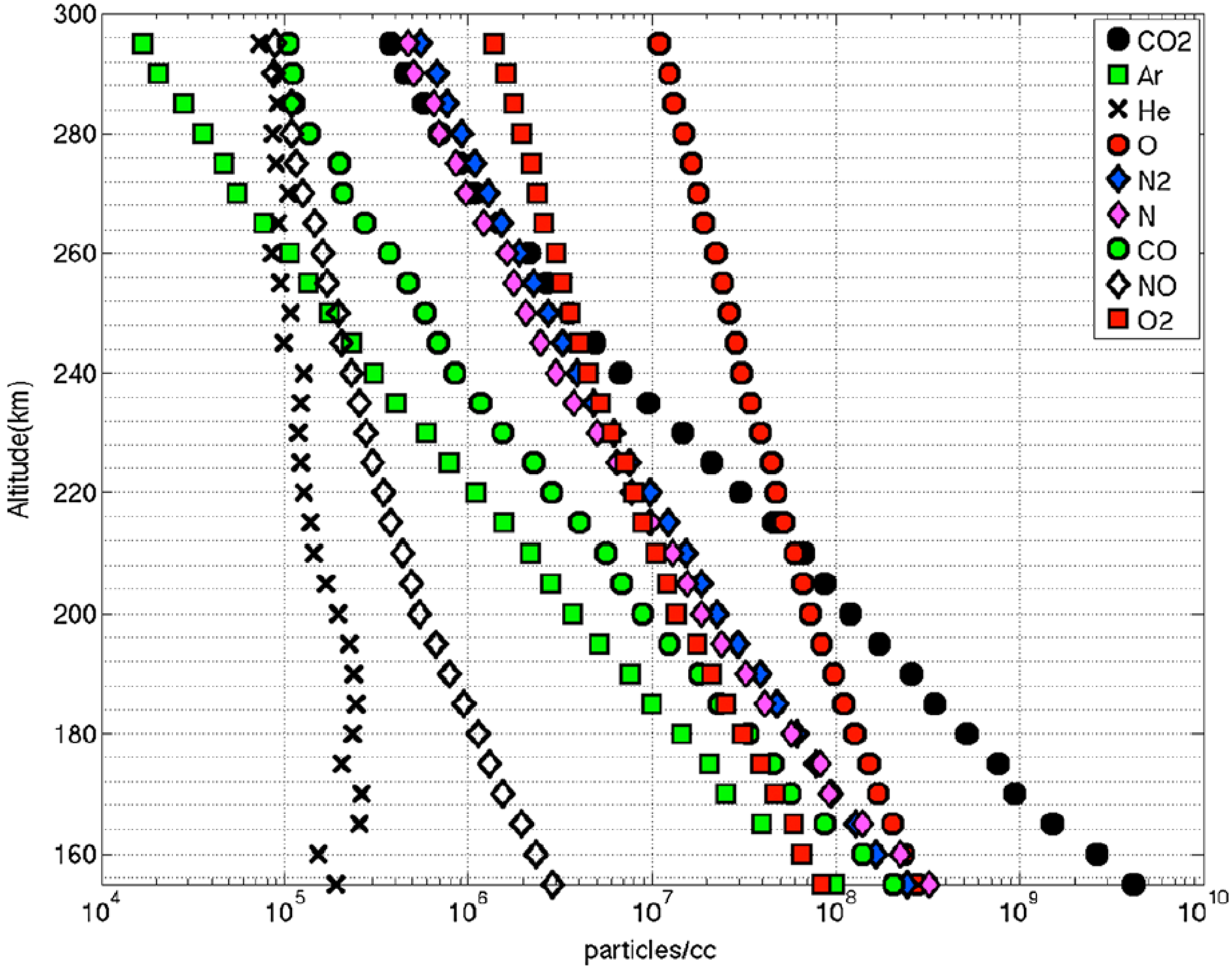

NO/N in the upper atmosphere

- Primary reaction $N_2 + h\nu \rightarrow N + N(^2D)$
- Main production NO: $N(^2D) + CO_2 \rightarrow NO + CO$
- Main loss process NO: $\mathrm{N} + NO \rightarrow N_2 + O$
- Ionospheric process: $NO^+ + e^- \rightarrow N(^2D) + O$
- At night $\mathrm{N} + O \rightarrow NO$

⇨ The remaining species is transported downwards into the Martian mesosphere.

Mm: Sporadic E / crustal magnetic field

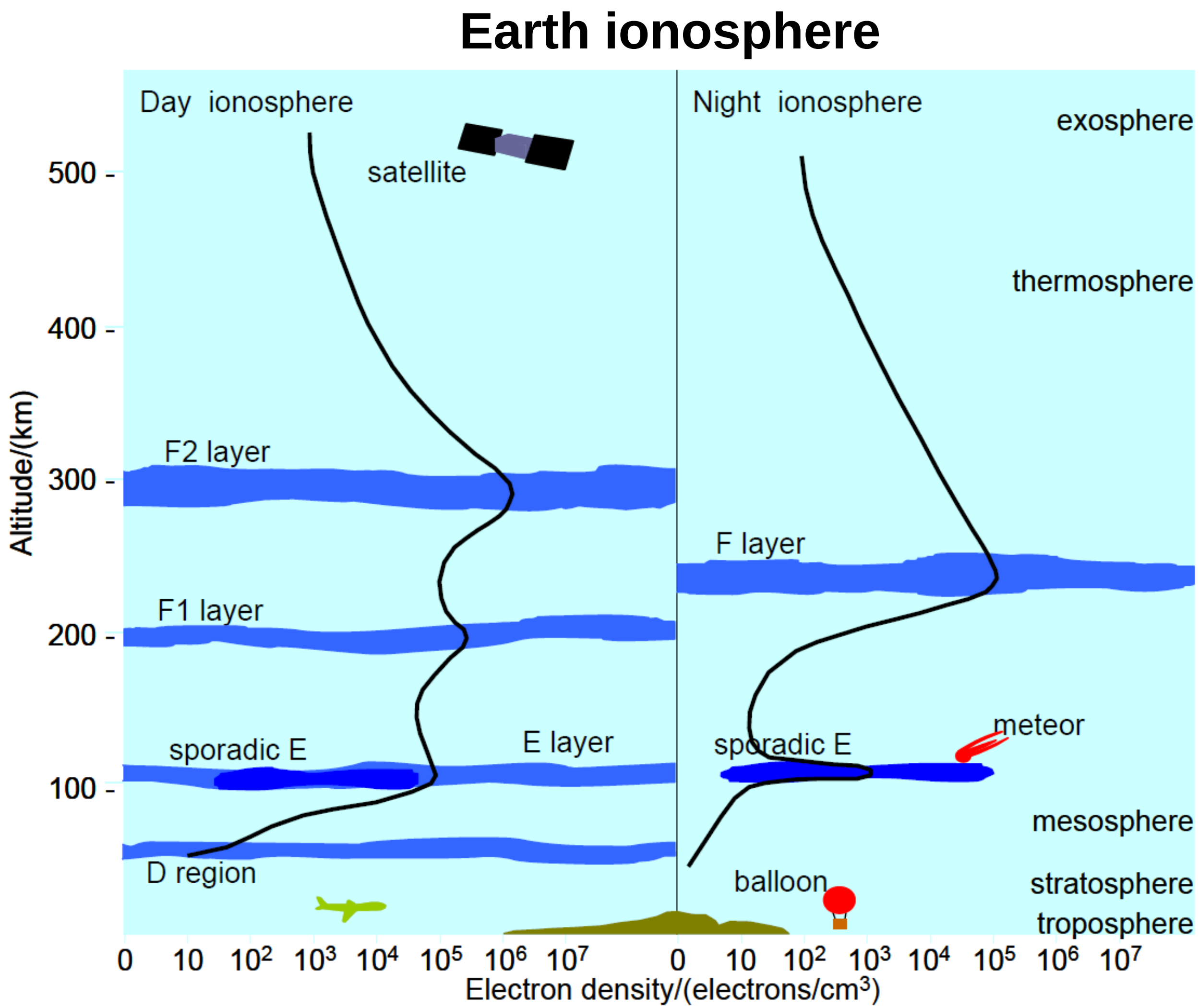

Introduction to HF radio propagation, IPS, (2008)

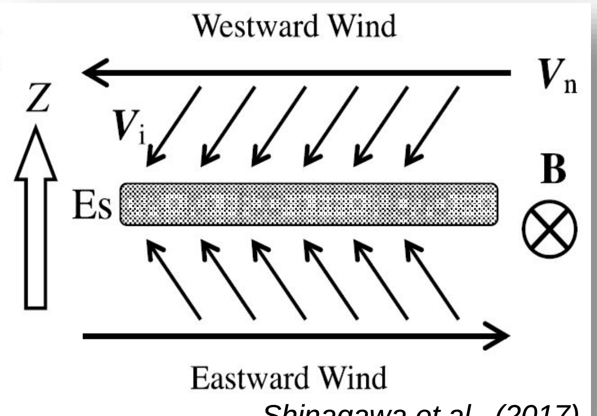

Shinagawa et al., (2017)

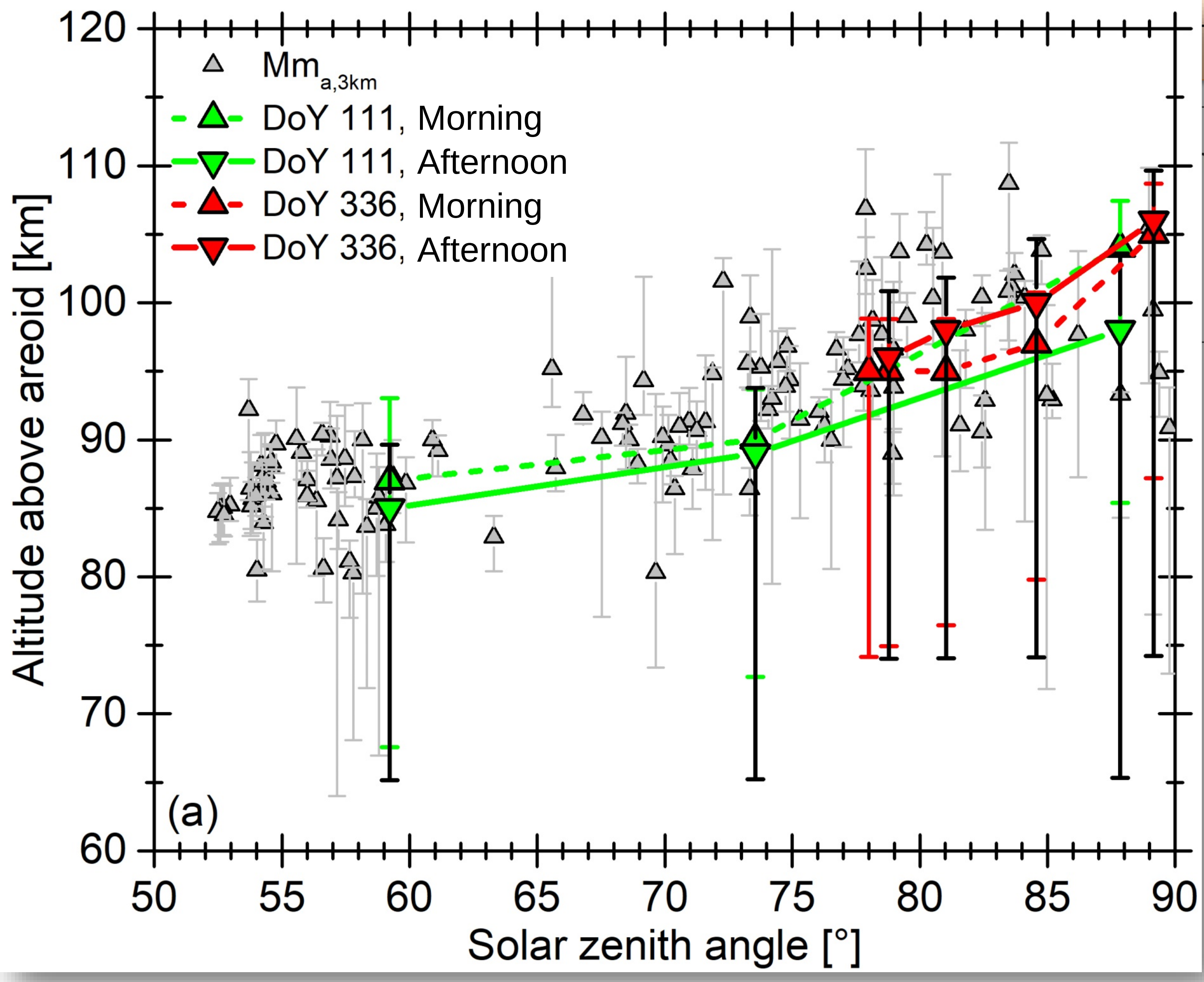

Mm a,3km
DoY 111, Morning
DoY 111, Afternoon
DoY 336, Morning
DoY 336, Afternoon
(a)
Altitude above areoid [km]
Solar zenith angle [°]